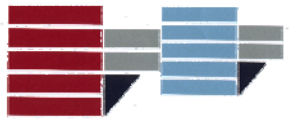

UNIVERSITÀ DELLA CALABRIA
"UNICAL"

Dottorato di Ricerca in

"**METODOLOGIE PER LO SVILUPPO DI MOLECOLE DI INTERESSE FARMACOLOGICO**" *XIX ciclo*

S.S.D. CHIM/08

Analytical Methods for Research and Development of Drugs

Coordinator
Prof. Giovanni Sindona

Ph.D. Student
Antonella Risoli

Supervisor
Prof. Gaetano Ragno

Anno Accademico 2005/2006

Index

INTRODUCTION

During the three hears of Ph.D. studies I dealt with different research lines, all set in the general research field of Analytical Pharmaceutical Chemistry.

In the first part, the studies were centered on the application of the technique QSPR (Quantitative Structure–Property Relationships) to a series of eleven antihypertensive 1,4-dihydropyridine drugs. These compounds are characterized by a high tendency to degradation when exposed to light, generating, in most cases, a related oxidation product. The influence of the substituents on the molecules, in terms of hydrophobic, electronic and steric effects has been investigated, defining a QSPR model able to correlate the degradation rate with the chemical structure of the drugs.

A second period of study was about the application of the Chemometric analysis on complex pharmaceutical matrixes, looking for analytical methods with higher trustworthiness than the conventional methods. On the spectrophotometric data obtained by the analysis of the drugs matrixes, PCR (Principal Component Regression) and PLS (Partial Least-Squares) algorithms were applied. The first step of calibration was in particular studied, trying to include different standard mixtures, presenting a changing number of components. The built models were optimized through the selection of the principal component numbers and the spectral region giving the more useful information; so all information about any others compounds, like excipients, could be deleted. SEP (Standard Error of Prediction) parameter has been chosen like the criterium for the definition of the model quality. The models have been validated on the same samples used in the calibration set and also on external series of synthetic mixtures.

Another study was centered on the determination of drugs, Trapidil in particular, in biological matrixes like serum and urine. In order to achieve both high sensitivity and selectivity, the drug from these complex matrices were isolated by Solid Phase Extraction (SPE). The analytical method was therefore defined by using the third-order derivative spectrum of the SPE eluate, which allowed the extraction of useful information and elimination of background absorbance. A signal in the third-order derivative spectrum was demonstrated to be directly proportional to the drug concentration and not influenced by matrix interferences. A linear regression equation was derived, which permitted the calculation of the analyte concentration from the absorbance signal.

The last year of the PhD was spent in a foreign stage, at the CRMS (Center for Research in Mass Spectrometry), York University, Toronto, ON, Canada. The studies were

about the development of a fragmentation hypothesis for a series of 1,4-benzodiazepines, a class of drugs widely prescribed. Analysis of these drugs is very important, due to their potential for addiction, abuse and overdose. Determination of a benzodiazepine by mass spectrometry (MS) is severely hindered by the lack of understanding of structure specific fragmentations. The research focused on MS fragmentations of thirteen drugs, with the purpose of eventually being able to predict the structure of an unknown 1,4-benzodiazepine from its mass spectrum and also with the purpose to create a library for these class of drugs.

1. STRUCTURE–PHOTOSTABILITY RELATIONSHIPS ON 1,4-DIHYDROPYRIDINE DRUGS

Quantitative-Structure Property Relationships (QSPR) techniques help to establish a correlation between the molecular structure and chemical or chemical-physics properties of compounds [1].

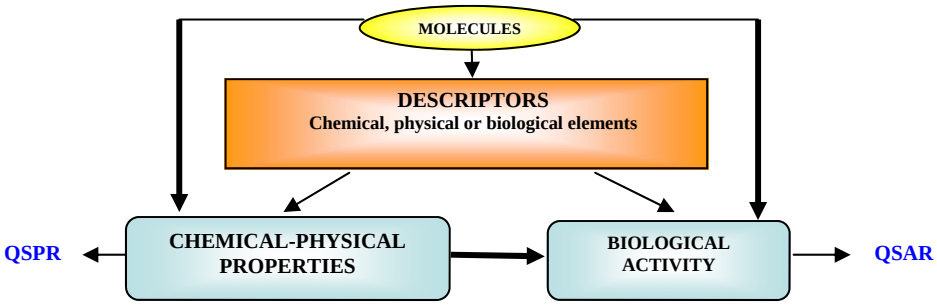

In a series of chemical structures, the relationship between chemical or chemical-physical properties (P) and various parameters or Descriptors (D), can be expressed by the equation:

$$P = a_1D_1 + a_2D_2 + a_3D_3 + \ldots\ldots a_nD_n + b$$

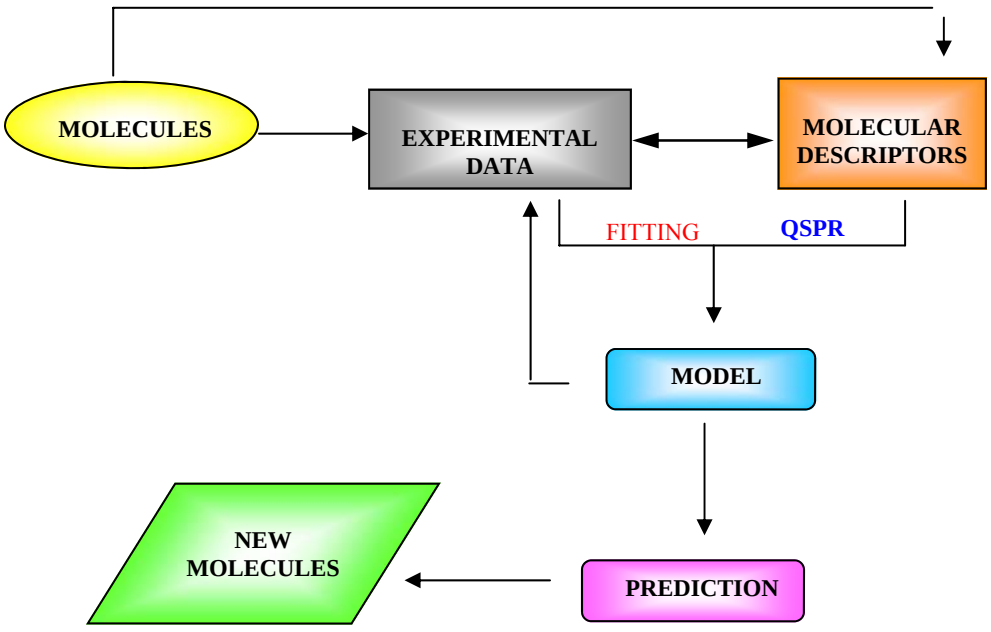

A QSPR model able to correlate the degradation rate and chemical structure of the 1,4-dihydropyridine drugs is herein proposed. The influence of the substituents on both phenyl and pyridine rings, in terms of hydrophobic, electronic and steric effects has been herein investigated [2]. A QSPR model able to correlate the degradation rate and chemical structure of the drugs was therefore defined.

Compounds	R_1	R_2	R_3	R_5	R_6
Amlodipine	$CH_2OCH_2CH_2NH_2$	$COOC_2H_5$	$COOCH_3$	Cl	H
Felodipine	CH_3	$COOCH_3$	$COOC_2H_5$	Cl	Cl
Isradipine	CH_3	$COOCH_3$	$COOCH(CH_3)_2$	Ossimidazolo	
Lacidipine	CH_3	$COOC_2H_5$	$COOC_2H_5$	$C(COOC(CH_3)_3)H=CH_2$	H
Lercanidipine	CH_3	$COOC(CH_3)CH_2N(CH_3)CH_2CH_2CH(Ph)_2$	$COOCH_3$	H	NO_2
Manidipine	CH_3	$COOCH_3$	$COOCH_2CH_2$-Piperazin-$CH(Ph)_2$	H	NO_2
Nicardipine	CH_3	$COOCH_3$	$COO(CH_2)_2N(CH_3)CH_2Ph$	H	NO_2
Nifedipine	CH_3	$COOCH_3$	$COOCH_3$	NO_2	H
Nimodipine	CH_3	$COOCH(CH_3)_2$	$COOCH_2CH_2OCH_3$	H	NO_2
Nisoldipine	CH_3	$COOCH_3$	$COOCH_2CH(CH_3)_2$	NO_2	H
Nitrendipine	CH_3	$COOCH_3$	$COOC_2H_5$	H	NO_2

The proposed model could be used to predict the chemical behaviour of new 1,4-dihydropyridines, virtually characterized by a high light stability.

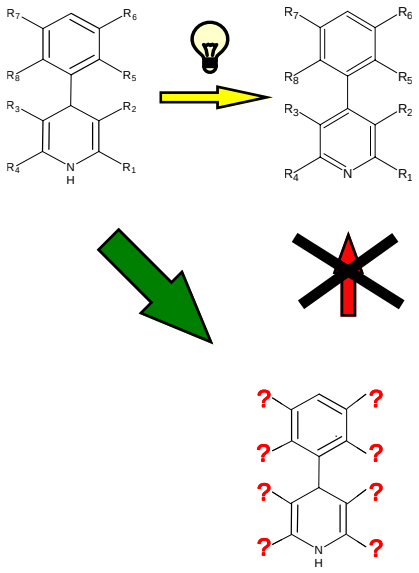

1.1 PHOTODEGRADATION KINETICS

The degradation study was performed by using a cabinet equipped with a Xenon lamp, which closely simulates sunlight. A comparison was performed by exposing compounds directly to sunlight and Xenon lamp, supplied with a UV-Glass and ID65 filter. The photodegradation process was monitored by spectrophotometry. Photodegradation studies have been performed in accordance with the "International Guide on Stability Study of New Pharmaceutical Substances and Products" published in 1993 from the Institute ICH (International Conference on Harmonization) and adopted in Europe, Japan and the United States.

Absorption spectra were recorded on a λ range of 190–400 nm in a 10mm quartz cell, by a Perkin-Elmer Lambda 40P spectrophotometer at the following conditions: scan rate 1 nm/s; time response 1 s; spectral band 1 nm; data density 1 point/nm. The software UV Winlab 2.79.01 (Perkin-Elmer) was used for spectral acquisition and elaboration.

Degradation of all the drugs were studied:

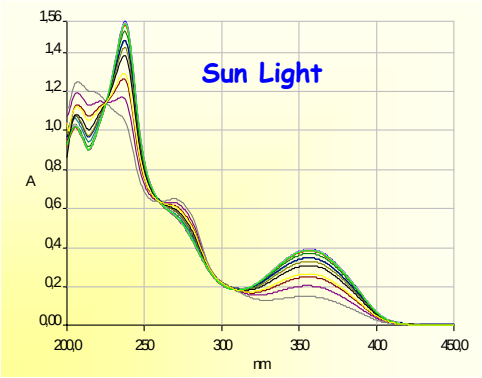

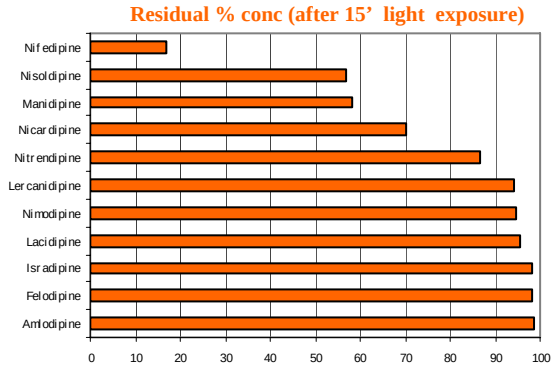

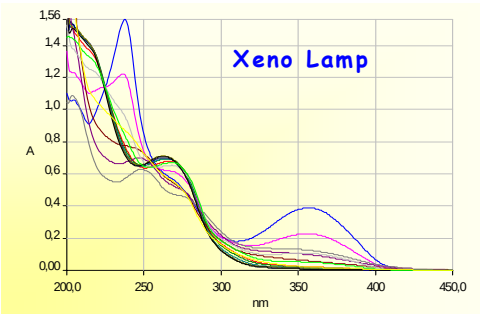

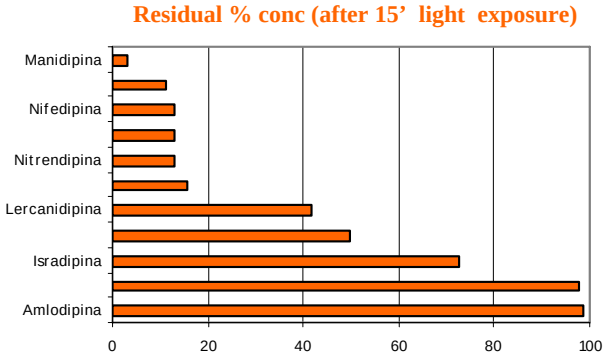

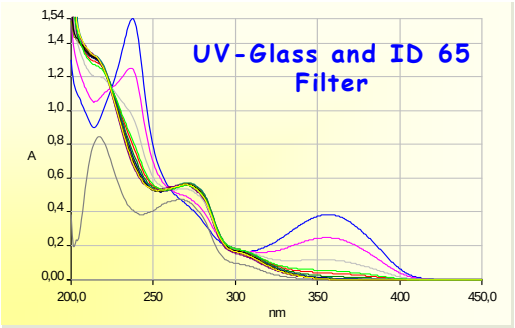

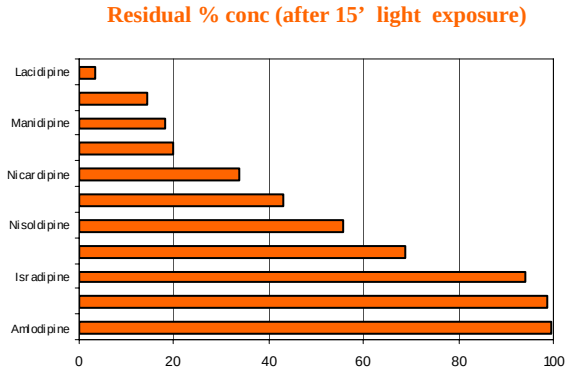

We tried to obtain as more information was possible from the degradation time and from the substituents in the different molecules, looking for a relationship between the various parameters studied.

1.2 PHOTOSTABILITY—DESCRIPTORS RELATIONSHIP

DESCRIPTORS

- ***log*P** — **Hydrophobic parameter**
- **σ** — **Electronic parameter**
- **τ** — **Steric parameter**

COMPOUNDS	residual % conc	R_5		R_6		
		σ	τ	σ	τ	*log*P
Amlodipine	99,57	0,67	3,52			3,22
Felodipine	98,89	0,67	3,52	0,47	3,52	3,3
Isradipine	94,18					4,15
Lercanidipine	68,78			0,71	3,44	4,18
Nisoldipine	55,72	1,72	3,44			4,18
Nitrendipine	42,88			0,71	3,44	4,2
Nicardipine	33,6			0,71	3,44	4,5
Nifedipine	19,85	1,72	3,44			4,53
Manidipine	17,84			0,71	3,44	4,8
Nimodipine	14,53			0,71	3,44	4,96
Lacidipine	3,55					5,56

A Multiple Linear Regression Analysis (MLRA) was applied to the calculated and experimental data, giving a multivariate model with good correlation values:

$$\%C = 356.606 + 8.406\,\sigma R_5 - 16.636\,\tau R_5 - 152.914\,\sigma R_6 + 21.664\,\tau R_6 - 63.387\,\log P$$

$$(r^2 = 0.9646)$$

where σ and τ represent the electronic and steric parameters of the chemical groups in meta or ortho position of the phenyl ring, respectively.

PHOTOSTABILITY- *log*P RELATIONSHIP

residual % conc = -0,0171 *log*P + 5,1781
R^2 = 0,8166

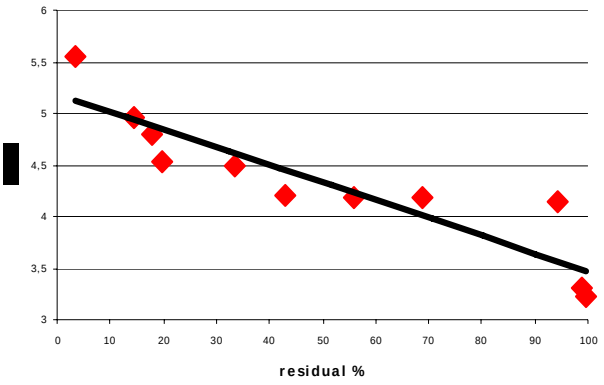

The equation obtained by multiple regression could be a good model for the prediction of 1,4-dihydropyridine drugs photostability on the basis of substituents nature. The verification that *log*P, a descriptor of the overall characteristics of a molecule, correlates with the photostability of drugs of this class confirmed this hypothesis.

The proposed model could be applied to the prediction of the chemical behaviour of new 1,4-dihydropyridine drugs virtually characterized by a high degree of light stability.

2. MULTIVARIATE CALIBRATION TECHNIQUES APPLIED TO THE SPECTROPHOTOMETRIC ANALYSIS OF ONE-TO-FOUR COMPONENT SYSTEMS

Multivariate chemometric methods seem to be the techniques showing a best performance in terms of complex mixture resolution [3–9]. Spectrophotometry has benefited after the introduction of chemometric procedures and several applications on pharmaceutical preparations, containing many active compounds and excipients absorbing in the same region, have been reported [10–15]. The application of these techniques on spectral data offers a main advantage which consists of speeding up complex systems resolution, without tedious preliminary separation steps. In fact, alternative techniques of wide application (i.e. liquid and gas chromatography), often result rather time consuming in the preparation and analysis of samples.

Among the various chemometric approaches applied to multicomponent analysis, principal component regression (PCR) and partial least-squares regression (PLS) have been successfully adopted in many quantitative assays of pharmaceutical formulations [16–20]. PCR and PLS are factor analysis methods which allow to establish a relationship between matrices of chemical data. The theory of such techniques has been fully described by several authors [21–25].

This report describes the resolution of a quaternary mixture containing paracetamol (PAR), caffeine (CAF), tripelenamine (TRP) and salicylamide (SAL) by the application of both PCR and PLS procedures to the absorption spectral data.

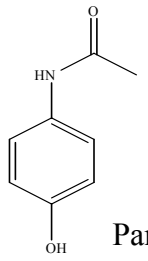

Paracetamol

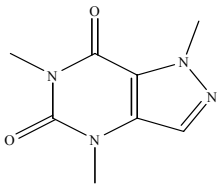

Caffeine

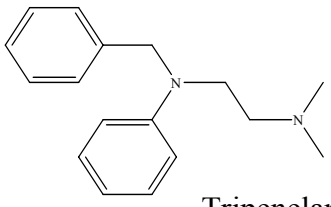

Tripenelamine

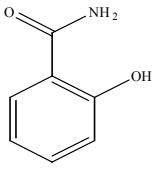

Salycilamide

The above drugs are combined all together only in one pharmaceutical speciality marketed in Italy, but they are also present in many analgesic and antipyretic formulations in different combination. The final goal of this study was the development of multivariate calibration algorithms able to quantify the above mentioned drugs not only in quaternary mixtures, but also in ternary and binary mixtures as well as single-component samples. For this aim, the planning of an experimental design was necessary to define a calibration set suitable for all drugs combinations.

The definitive models were drawn after a carefully selection of the wavelength regions to be used in calibration, so ensuring either an acquisition of useful information and a removal of redundant or noisy data.

Absorption spectra were recorded on a λ range of 190–400 nm in a 10mm quartz cell, by a Perkin-Elmer Lambda 40P spectrophotometer at the following conditions: scan rate 1 nm/s; time response 1 s; spectral band 1 nm; data density 1 point/nm. The software UV Winlab 2.79.01 (Perkin-Elmer) was used for spectral acquisition and elaboration.

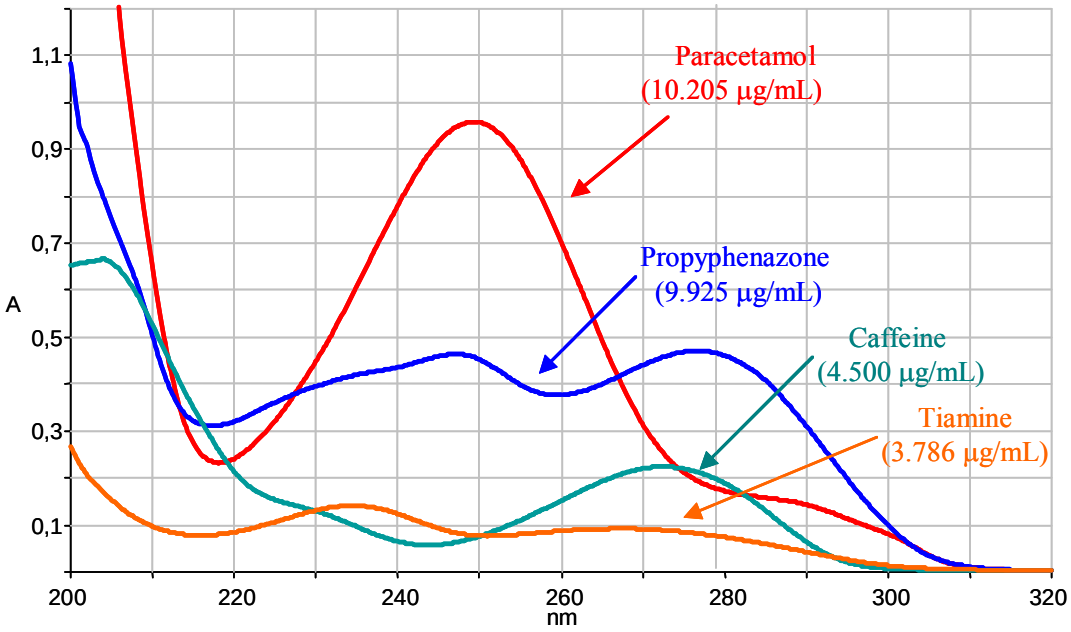

. Experimental design was carried out by using the software Unscrambler v.6.0. PAR, SAL, TRP and CAF were a generous gift from Ogna SpA, Italy. The pharmaceutical specialities Anticorizza® (Ogna SpA, Italy), Acetamol® (Abiogen Ph, Italy), Efferalgan 1000® (UPSA SpA, Italy) were obtained commercially. Stock solutions in ethanol, of the four studied drugs were used to set up the calibration set. These stock solutions were appropriately diluted to give reference solutions with concentrations within the range 5.0–

25.0 μgml for PAR and SAL, and within 0.5–5.0 μgml for CAF and TRP. PCR and PLS analysis were performed by using the dedicate software Quant+ 4.01 (Perkin-Elmer). The software permits to validate the models by independent validation or full cross-validation. In the first procedure, selected references are removed from the training set before the calibration was performed, then predicted against the calculated calibration. In full cross-validation, iterative calibrations are performed removing in turn each standard from the training set and then predicting the excluded sample with that calibration

The external validation of the calibration models was achieved over the spectra of a prediction set consisting of 19 synthetic mixtures containing one-to-four component in different ratios, with concentrations within the ranges used for the standard solutions.

For the assay of the commercial formulations, five tablets were weighed and reduced to a fine powder. An amount corresponding to the average of tablets contents was accurately weighed, then diluted to a volume of 50 ml with ethanol-NaOH (1.2×10.4 M; pH 10). The suspension was sonified for 10 min and then filtered through a PTFE 0.45 μm membrane filter. One milliliter of this filtrate was diluted to 200 ml with ethanol and analyzed. The values were chosen in agreement with the concentration ratios present in the investigated commercial formulation.

Multivariate calibration consists of the establishment of a relationship between matrices of chemical data. The methods are based on a first calibration step in which a mathematical model is built, using a chemical data set (e.g. absorbance values) and a concentration matrix data set. The calibration is followed by a prediction step in which this model is used to estimate unknown concentrations of a mixture from its spectrum. In particular, PCR and PLS techniques are called “factor methods” because transform the high number of original variables into a smaller number of orthogonal variables called “factors” or “principal components”, which are linear combinations of the original variables. The first factors contain useful information, whereas the last ones represent the noise, which has to be discarded and not considered in the modeling.

The selection of the optimal number of factors used to build PCR and PLS models represents a decisive step to improve the prediction power of the methods. A full cross-validation, also called leave-one-out cross-validation, was employed towards this aim. It consists of removing one sample at a time from the calibration step and performing the calibration with all other samples. The concentration of the sample removed is then predicted with the obtained model. This step is in turn repeated for each sample considered. The procedure can be repeated after fixing a different number of factors. The

standard error prediction (SEP) was chosen as an optimizing criterion to select the optimal number of factors. SEP represents an estimate of the error involved in the assay of external samples by using the model. Its value depends on the number of factors used for that calibration. The number of factors giving the minimal SEP was selected as the optimal number of factors.

SEP was calculated by means of the following expression:

Chemometric Parameters

Standard error of prediction (SEP)

$$SEP = \sqrt{\frac{\sum (\bar{y} - y)}{n-1}}$$

Standard error of estimate (SEE)

$$SEE = \sqrt{\frac{RSS}{n_{stand.} - n_{factors} - 1}}$$

Multiple correlation coefficient (R)

$$R = \sqrt{1 - \frac{RSS}{TSS}} \qquad TSS = \sum_i \left(y_i - \bar{y}\right)^2$$

TSS = Total sum of squares

Determination coefficient
R^2

RSS = Residual sum of Square

$$RSS = \sum_i (y_i - \hat{y})^2$$

where y_i/ i is the predicted concentration value of the i^{th} calibration sample and y_i is its real concentration. The *F*-test between two consecutive factors, able to point out if their difference is caused by real variation rather than noise in the spectral data, was used to determine the significance of SEP values greater than the minimum. The optimal number of factors was determined according to Haaland and Thomas [10], which proposed an *F*-ratio probability of 0.75 as a good choice.

The analysis by ordinary or derivative spectrophotometry, using measurements at discrete wavelengths, could not be satisfactorily performed because of the extensive overlap of the peaks. The spectral interference resulted very critical for CAF and TRP, because of the relatively higher concentration of the two other components. Multivariate calibration methods appeared then to be ideal in order to provide an effective solution to this problem, as they allow to extract analytical information from the full-spectra of multicomponent samples. However, if not every wavelength provides useful information, an optimal selection of the wavelength regions used in calibration must be considered to improve the model.

Besides a carefully selection of the wavelengths, an appropriate design of the calibration set to be used in modelling was taken into account during elaboration of the analytical procedure.

Multivariate calibration methods, such as PCR and PLS, require a suitable experimental design for defining the calibration set, in order to keep a lowest number of samples and to arrange these homogeneously in the experimental domain. A training set of 25 quaternary mixtures was prepared, selected according to a three-level experimental design based on a central composite design (CCD). The ranges of the concentrations were selected in order to keep the same ratios of the drugs as in the available pharmaceutics.

Special care was taken to ensure that, in the concentration ranges studied and for all the mixtures, either the total absorbance did not exceed the linear range of the spectrophotometer and the contribution of each component was additive. The PCR and PLS models obtained by using this training set were validated by full cross-validation and the SEP values were calculated each time that a new factor was added to the models. As can be seen, the prediction values for PAR and SAL in both models is good, with SEP values under 1.0 and R_2 above values of 0.98. Wrong results were collected for CAF and TRP in terms of either SEP and R_2. A possible explanation for the higher errors in CAF and TRP prediction is probably due to the low content of these components in the reference mixtures and this could result in poor information from the spectral data.

One set of 19 synthetic samples, containing quaternary, ternary, binary and single component mixtures of the four concentrations (μg/ml) of references solutions in calibration set A, studied drugs, in different ratios, was built to perform an external validation for the defined PCR and PLS models. The construction of the prediction set was defined to test the prediction ability of the models (built with quaternary mixtures only), when applied on samples with a number of components less than four. The mixtures were prepared in the same concentration ranges used in the calibration set A. In particular, the ternary and quaternary mixtures were made in such a way to include all the three concentration levels used in that calibration set, whereas in binary and single-component mixtures only the upper and lower levels were selected.

When the calibration models were applied to the prediction set, different results were obtained. Good results were carried out from prediction of the quaternary mixtures, with a mean accuracy, expressed as percentage recovery (±R.S.D.), of 102.45 (±2.29) and 98.56 (±1.41), for PCR and PLS, respectively. On the contrary, very poor results were obtained from analysis of one-to-three component samples, with mean residual errors above 10%.

Moreover, the models showed to be particularly defective in predicting the zero concentration of the absent components, carrying out improper contents of these above 5–10%. The failure of the models, when applied on mixtures containing a number of components below four, was supposed to be caused by the partial data information provided by the calibration set A, containing quaternary mixtures only. Thus, it seemed convenient to increase the first calibration set with the addition of ternary, binary and one-component mixtures, in order to provide further information concerning these samples composition.

The attempt to build the postulated calibration set by several proved experimental designs failed. Only CCD, which was already adopted to generate the calibration set A, proved to be suitable for obtaining one-to-three component mixtures, by fixing a zero concentration value for each component, even though only a two-level design could be obtained in such a way. Therefore, a new calibration set B was manually built in order to keep a three-level system on. Same concentrations as for calibration set A were used and the matrix was accordingly built in order to retain a homogeneous distribution of all concentration levels. New PCR and PLS calibration models were then developed by using simultaneously the spectral data from all the 47 mixtures of the calibration sets A and B.

Concentrations (μgml) of references solutions in calibration set B, by full cross-validation of the models did not result significantly different from the ones provided by calibration set A only. A slight increase of the correlation coefficients was always observed, showing a good accordance between predicted and known concentration values for the overall data set.

On the contrary, the application of such models to the prediction set allowed a remarkable improvement of the results. All the estimated concentration values were predicted with a residual value of less than 2.4% and the mean accuracy, expressed as percentage recovery (±R.S.D.), was found to be 101.67 (±1.95) and 100.62 (±1.59), for PCR and PLS, respectively, with all the mean residual errors above 4%.

A large discrepancy between labeled amounts and experimental results were obtained when the above models were applied to the analysis of a quaternary pharmaceutical formulation.

In particular, the residual errors for the predicted concentrations of PAR and SAL ranged between 4 and 9%, whereas for TRP and SAL, whose content is very low if compared to the two other components, errors above 10% were obtained. This high

inaccuracy was supposed to be caused by bad information or noise in the spectral data, probably due to the unavoidable concomitant extraction of some excipients.

When the problem is represented by the presence of excipients having interfering absorbances, a selection of wavelength ranges seems to be convenient in order to emphasize spectral characteristics of the components of interest or de-emphasize features of other potentially interfering components. Although chemometric methods such as PCR and PLS are designated to be full-spectrum procedures, a selection of wavelength subsets is often recommended for multicomponent systems presenting severe overlapping in UV spectra [26–30]. As a first correction, the wavelength zone below 210 nm was rejected, because the signals there found were verified to be characterized by higher variance than the rest, furnishing only noisy information for the algorithm. Analogously, the range over 340 nm was discarded, because of the absence of useful information. Calibration was then re-calculated by using the wavelength range 210–340 nm only. Assay results obtained by applying the new PCR and PLS models resulted yet scantly improved with respect to those calculated by using the full-range spectrum. In the subsequent step, the potential interference of the excipient rosin was investigated, because of its relative low solubility in ethanol (used as extraction medium from tablets). Rosin absorbs between 230 and 255 nm, overlapping with the main absorbance bands of SAL and TRP. The calibration was so iteratively re-calculated after the elimination of a narrow spectral range at a time between 230 and 255 nm. The best improvement in the accuracy of the predicted concentrations for all the components in the pharmaceutical specialty was achieved when the 230–245 nm wavelength range was discarded and only the 210–229 and 246–340 nm ranges were used to build the calibration models.

Cross-validation of the final models was performed with respect to the number of factors affecting the prediction of each of the compounds. The optimum number of factors was found to be four for SAL and TRP, six for PAR and seven for CAF in the PCR model, while the optimum number of factors was found to be six for SAL and TRP, seven for PAR and five for CAF, in the PLS method

The concentrations predicted by the models were found to be very close to the nominal concentrations, confirming the validity of both methods. The obtained results were not significantly different from those obtained in the previous models based on the full spectral data, so demonstrating that the discarded 230–245 nm zone does not contain significant information. The prediction ability of both PCR and PLS methods was demonstrated by the good results obtained in terms of accuracy and precision. The mean recovery resulted

within 97 and 103% and precision, expressed as R.S.D., was calculated to be always under a 5%.

The selection of the wavelength ranges allowed a significant reduction of the errors in assaying the pharmaceutical samples. In the analysis of tablets, recoveries were in a fairly good agreement with labeled contents, and precision was calculated within 1.0–5.0% for both multivariate methods.

No significant differences in results were obtained when PCR and PLS models were applied to the prediction of synthetic mixtures, thus proving a high resolving power for both chemometric methods in the analysis of multicomponent complex mixtures. Moreover, both procedures gave results in agreement with the labeled drugs content when applied on pharmaceutics. PLS seemed to be a little more sensitive in the case of an extensive spectral overlap. Actually, CAF and TRP determination, which were present in a very low concentration compared to the larger amounts of PAR and SAL, showed slightly better results, in terms of accuracy and precision, by using the PLS model.

PCR accounts for all the spectral data simultaneously and then, in a second step of multiple regression, correlates these with the components data. On the other hand, PLS provides to individually analyze each component by correlating the variation in the component information with respect to the spectral data. Therefore, even a slight difference in the variable data, like the absorbance of components present in small amounts, is taken into account for producing a more robust model with greater predictive power than the calibration model constructed using PCR.

Nominal				Found							
				PCR				PLS1			
PAR	PRO	CAF	TIA	PAR	PRO	CAF	TIA	PAR	PRO	CAF	TIA
Prediction set											
5,103	-	-	-	5,102	-0,081	0,025	0,015	5,097	-0,102	0,044	1,033
-	9,925	-	-	0,032	9,978	0,066	-0,134	0,008	10,020	0,054	1,064
-	-	1,125	-	-0,020	-0,081	1,133	0,027	-0,039	-0,045	1,102	1,004
-	-	-	2,524	-0,010	-0,013	-0,015	2,648	-0,017	0,050	-0,025	1,008
-	9,925	-	2,524	0,019	10,050	0,013	2,286	0,059	10,050	0,036	1,071
30,615	-	4,500	-	30,580	0,116	4,419	-0,081	30,570	0,200	4,441	1,224
10,205	-	-	3,786	10,090	0,043	-0,052	3,762	10,130	-0,018	0,036	1,080
-	14,888	0,563	-	0,055	15,090	0,544	-0,100	0,060	15,100	0,551	1,098
10,205	-	0,563	2,524	10,210	-0,035	0,527	2,476	10,220	-0,082	0,567	1,079
-	14,888	0,563	3,786	0,006	14,670	0,592	3,576	0,020	14,720	0,563	1,108
20,410	19,850	0,563	-	20,380	19,790	0,590	0,055	20,380	19,730	0,591	1,266
30,615	4,963	-	2,524	30,680	5,007	0,015	2,362	30,610	4,942	-0,061	1,244
5,103	9,925	4,500	1,262	5,010	9,813	4,510	1,260	5,005	9,784	4,526	1,122
10,205	4,963	1,125	0,631	10,140	4,928	1,072	0,613	10,120	4,887	1,073	1,106
10,205	19,850	2,250	2,524	10,240	19,940	2,326	2,560	10,230	19,920	2,235	1,214
5,103	9,925	4,500	0,631	5,070	9,859	4,488	0,701	5,049	9,842	4,493	1,121
Commercial formulations											
EFFERALGAN (Upsa)											
500	-	-	-	486.39	0.98	0.23	0.062	501.6	0.73	0.15	-0.085
BENERVA (Roche)											
-	-	-	100	0.99	0.53	0.074	97.98	1.03	0.65	0.088	98.23
SEDOL (Off.Farm.Fiorentina)											
-	500	50	-	1.04	479.25	48.96	0.018	0.86	518.10	47.75	0.054
SARIDON (Roche)											
250	150	25	-	248.23	146.51	26.31	-0.28	247.36	154.98	30.68	-0.62
ODONTALGICO DR KNAPP (Montefarmaco OTC)											
310	310	25	15	321.98	318.34	20.47	20.01	308.33	301.42	18.99	18.56

3. DETERMINATION OF TRAPIDIL IN SERUM AND URINE BY SPE AND DERIVATIVE SPECTROPHOTOMETRY

The triazolopyrimidine Trapidil (5-methyl-7-diethylamino-s-triazolo [1,5-α] pyrimidine), is a common antiplatelet drug knew in Italian marketing like Travisco®, used in ischemic Cardiopathy.

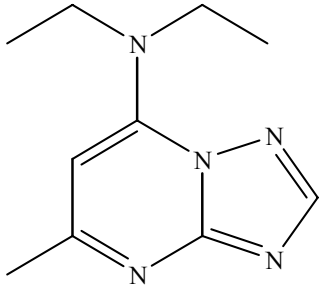

It's able to suppress some grow factors in several cells. In this way it may antagonize some platelet-derived grow factor (PDGF). This drug can also stimulate the prostacycline (PGI_2) production, but to the other side doesn't stimulate the tromboxane A_2 (TXA_2), and is also a non selective inhibitor of phosphodiesterases, with a consequentially increase of cAMP and an increasing of factor cAMP-dependent like the protein kinase A (PKA). The effects are coronary vasodilatation, antiischemic effects in vivo and in vitro, inhibition of vascular smooth muscle cell proliferation, antiplatelet and antiatherosclerotic action [31-33].

The first aim was to look for a method able to isolate with high accuracy and precision the drug from biological samples, like blood and urine. These matrixes are very complex because they have a lot of proteins and impurities that can give a lot of interferences, even after purification of the samples. We decided to use solid phase extraction (SPE) cartridges [34], but only Strata-X cartridges were very useful for the detection of Trapidil. These cartridges are based on a polymeric stationary phase that selectively interacts with the drug and eliminates most of the compounds that interfere with the analysis.

An attempt at sample extraction and drug preconcentration using a series of commercially available SPE cartridges was successful, with excellent results obtained. The principal role of the SPE cartridges is the retention of the analyte of interest from the sample and the elution of the interferences, in fact one of the common application of the SPE cartridges is the extraction of drugs from body fluids. The SPE reduces the handling of body fluids, such as blood and urine [34].

In the last time several techniques have been improved for sensitive and selective determination of drugs and metabolites from biological fluids by using SPE methods [35].

The aim of this work was to develop an analytical method to extract Trapidil with high precision and accuracy from the biological fluids. For the detection of the analyte the third-order derivative spectrophotometry was used for the direct assay of Trapidil in serum blood and urine [36-37].

Absorbance spectra were recorded at a data density of one point per nanometer in the wavelength range 200 - 800 nm, in 10 mm silica quartz cells, by means of a Spectrophotometer Lambda 40P (Perkin-Elmer) at the following instrumental conditions: scan speed, 1 nm/s; time response, 1 sec; spectral bandwidth, 1 nm. UV WinLab 2.70.01 package software (Perkin-Elmer) was used to acquire and elaborate the spectral data.

Trapidil was purchased from Chiesi Pharmaceutics SpA (Italy), Methanol and Water, were purchased from J.T. Baker (Holland), Travisco® (Chiesi Pharmaceutics SpA, Italy) was obtained commercially.

The complex matrixes, like serum and urine, have to use a necessary method to simplify the sample, which is able to increase the analyte concentration as well as to eliminate many different interferences. Strata-X cartridges were purchased from Chemtex Analytica (BO, Italy). Strata-X is a new, patent-pending sample preparation sorbent for a reversed-phase solid-phase extraction. The Strata-X 33μm polymeric sorbent offers a huge advantages over traditional silica-based sorbent chemistries.

The zero-order spectrum of the SPE eluate showed good resolution of the main peak of the drug, but with an unacceptable high, 5-10%, error range for the predicted concentration. The cause of this error was demonstrated to be the persisting presence of interferences incompletely eliminated in the extraction step.

The ordinary samples spectrum, obtained from SPE, shows a good resolution, but we have a low accuracy about the prediction of concentration values, with an excess error between 5-10%, due to the persisting presence of absorbance of noise, that we cannot eliminate completely during the extraction phase.

We calculated the maximum level of capability in the cartridge and the highest amount for an analytical determination was a concentration of 200 μg/mL, while the lowest amount was 0.1 μg/mL, the definition bound was 0.2 μg/mL.

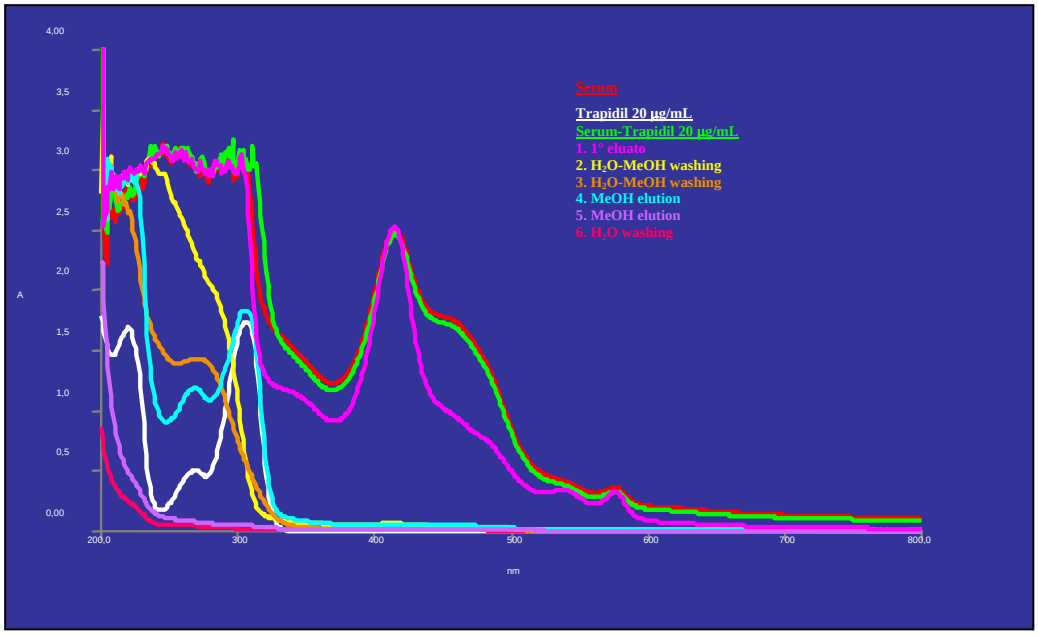

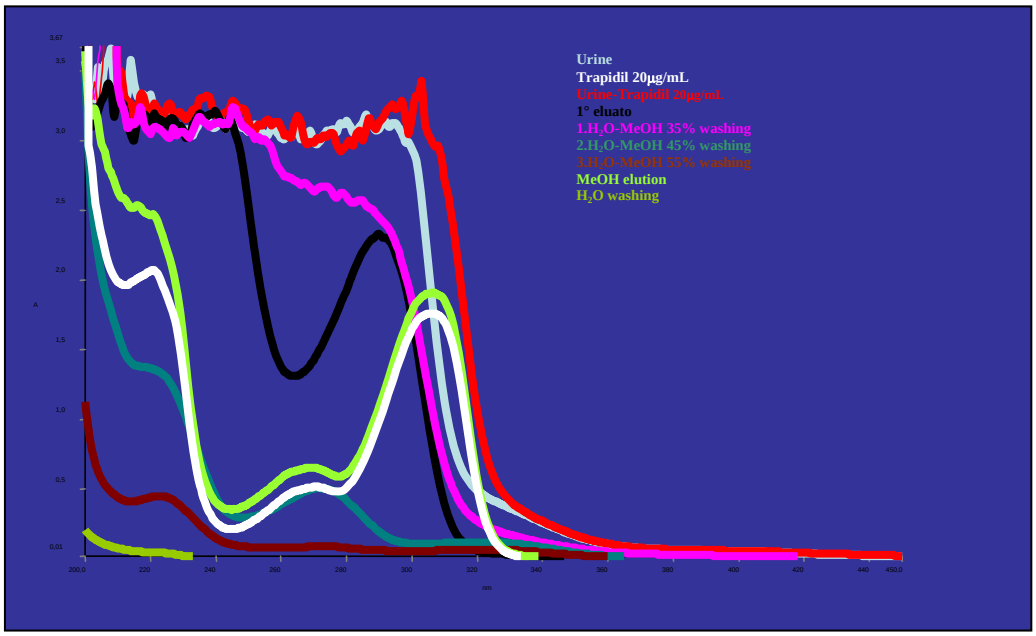

Both the parameters of sensitivity were considered satisfactory because we have to consider that the maximum blood concentration of the therapeutic supply of the drug is between 4 e 6 µg/mL [39].

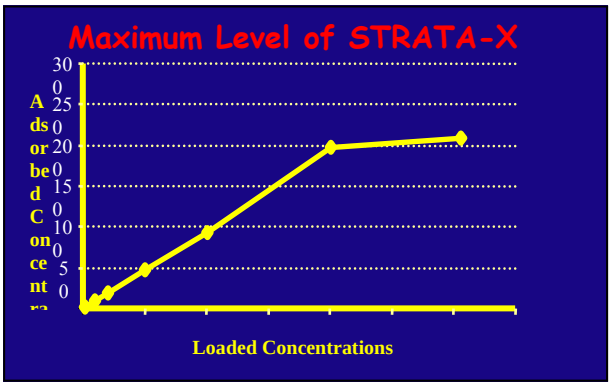

The analytical method was obtained with a third order derivative spectrophotometry, able to extract the useful informations of the SPE eluate and to eliminate the background of absorbance, due to the interferences typical in biological samples.

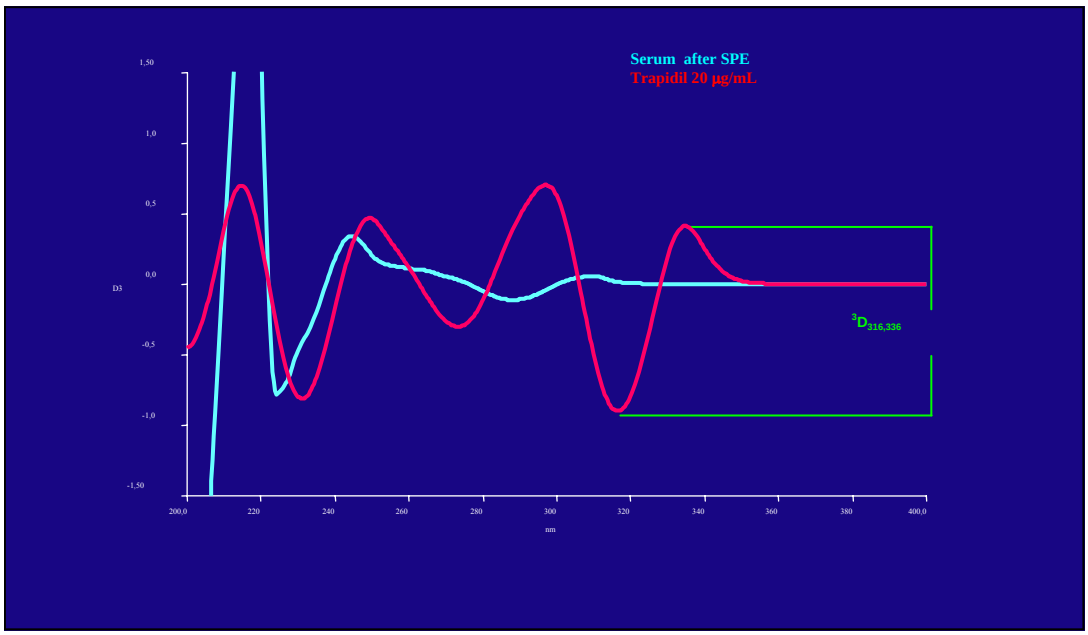

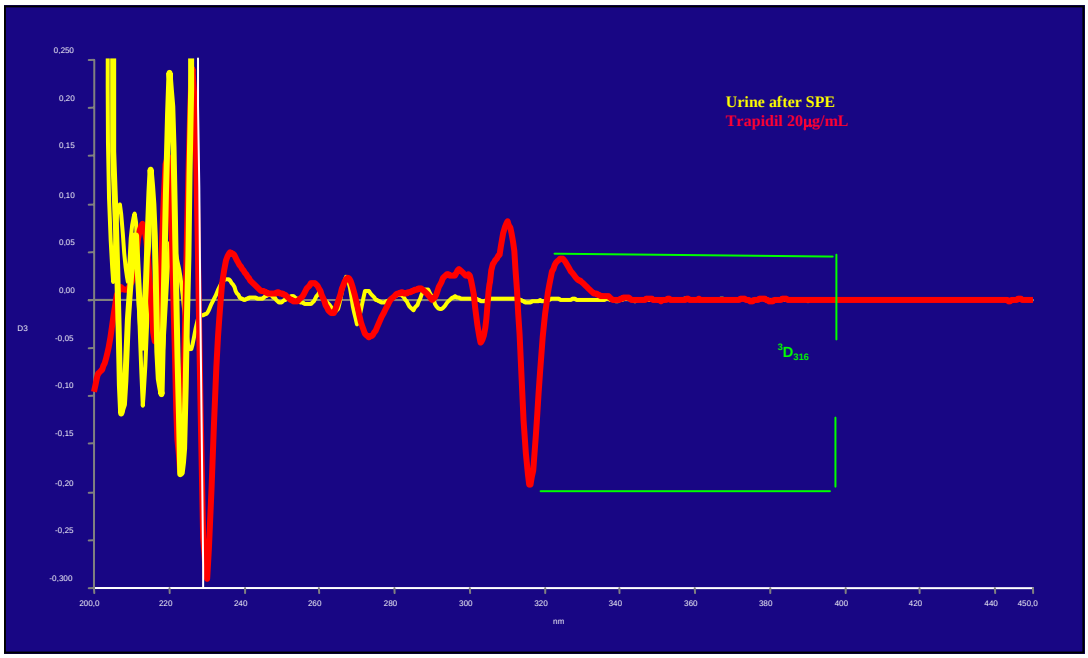

We isolated a signal from the spectrum of third order derivative spectrophotometry directly proportional to the drug concentration, without any extraneous absorbment.

In this way we defined a linear regressional equation able to directly correlate the analita concentration with the analytical signal of absorbance.

A generic sorbent must be able to trap a specific compound, and has also to be able to an efficient and complete desorption using the right solvents [38]. Maybe the difference was that the Strata-X had a bigger and stronger interaction due to the polymeric sorbent, that can interact selectively with a many kind of molecules with a lot differents hydrophobicity.

We started to analize the absorbance spectra, but even after the isolation of the drugs from the biological fluids we didn't have a clear isolation, in fact we always had some residual interferences from the biological matrixes. The analytical method was therefore further optimized by using the third-order derivative spectrum of the SPE eluate, which did allow the extraction of useful information and elimination of background absorbance. In fact after the purification with SPE, the biological fluids didn't have any D_3 absorbance in the drop 316.

The signal $^3D_{316,336}$ = 0,0673 [C] + 0,0027 of the third-order derivative spectrum in serum and the $^3D_{316}$ = 0,0735 [C] + 0,0032 of the third-order derivative spectrum in urine was demonstrated to be directly proportional to the drug concentration and was not influenced by any matrix interferences.

A linear regression equation for both the kind of samples (r_{serum} = 0.9998 and r_{urine} = 0,9799) were derived that permitted the calculation of the analyte concentration from the absorbance signal respctively.

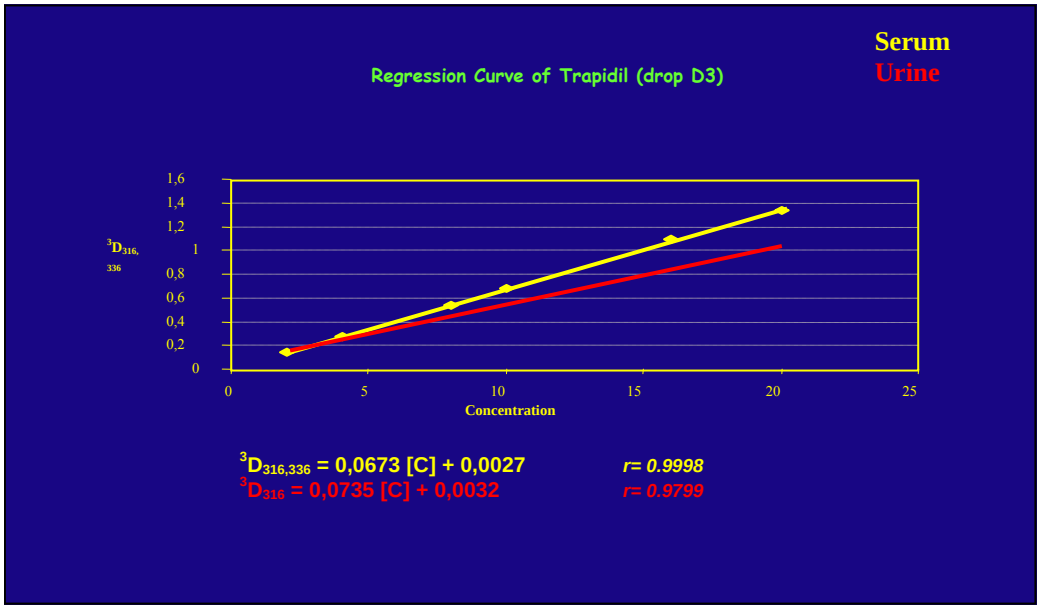

The accuracy and precision of the method was validated by comparison of standard extraction without any biological matrixes and only biological samples. The method showed a linear correlation for a 0.2 - 50 μg/ml concentration range.

In addition to satisfactory elimination of interfering compounds, SPE extraction also allowed a near 100% drug recovery from the stationary phase. The subsequent use of derivative spectrophotometry allowed the quantitation of Trapidil in human serum and urine with good accuracy and precision.

Dosage of Trapidil in Serum with Strata-X cartridges

Real Concentrations	Drop $D3_{316,334}$	Calculated Concentrations	E%
0,5021	0,03307	0,4752	5,357499
2,0084	0,14482	2,1017	4,645489
5,021	0,31966	4,7097	6,19996
10,042	0,63796	9,71948	3,211711
15,063	0,96246	14,367	4,620726
20,084	1,28068	19,7894	1,467088

Dosage of Trapidil in Serum

Accuracy (% recovery) = > 96 %

Precision (RSD) = < 4%

Dosage of Trapidil in Urine with Strata-X cartridges

Real Concentrations	Drop $D3_{316}$	Calculated Concentrations	E%
0,501	0,00430	0,568	10,45
2,006	0,02275	2,131	4,23
5,010	0,05368	4,753	3,12
10,032	0,10429	9,041	3,87
20,064	0,24587	21,040	2,86

Dosage of Trapidil in Urine

Accuracy (% recovery) = > 95 %

Precision (RSD) = < 4,5%

The extraction with SPE has been a very good method to isolate selectively the drug from biological samples, like Serum and Urine. As well the stationary phase has a very important role in order to obtain a quantitative drug recovery and a complete elimination of interferences.

The last generation cartridges (Strata-X) is an excellent tool to selectively extract the drug, in fact we obtained the highest recovery percentage.

The application of derivative spectrophotometry allowed the analytical determination of the drug and its precision. We obtained the precise determination of the analite with high statistical performance, with the isolation of a drug signal characteristic, without any interferences, and at the same time it has been possible to eliminate the noise absorption, which is typical for the complex matrixes like biological samples.

The combination of both these techniques, the SPE and the derivative spectrophotometry, has allowed the analita determination with an accuracy superior than 96% in Serum and 95% in Urine.

The selectivity of the drug extraction in the biological matrixes allowed a quantitative identification of the drug concentration for possible pharmacokinetics studies.

4. DEVELOPMENT OF A MASS SPECTRAL LIBRARY FOR PREDICTION OF FRAGMENTATION PATHWAYS OF BENZODIAZEPINES

The 1,4-Benzodiazepines (**Fig.1**) are widely prescribed drugs [40]. Benzodiazepines represent a class of sedatives and tranquillizers commonly used to produce sedation, induce sleep, relieve anxiety and muscle spasms, and prevent seizures [40,41]. The analysis of these drugs is important for pharmacological and toxicological studies as well as in clinical forensic and law enforcement applications due to the their addictive potential [41].

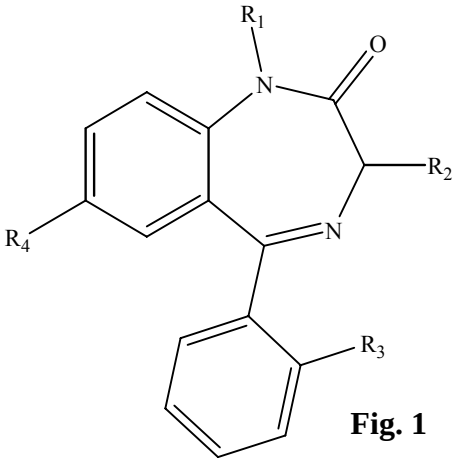

Fig. 1

A variety of methods exists for detection and determination of 1,4-benzodiazepines in biological matrices, but none of the existing methods equals the sensitivity of mass spectrometry based methods [42]. The primary focus of published mass spectrometric studies has been to correlate fragmentation pathways to structural features of 1,4-benzodiazepines and their metabolites. In a study based on electron impact (EI) induced fragmentation of 1,4-benzodiazepines, the molecular ions fragmented mainly by loss of CO, HCN and HCO to form a smaller ring system [40].

A large number of papers using mass spectrometry for the determination of 1,4-benzodiazepines are devoted to their detection and quantitation in biological matrices [43,44,45,46], but only limited number of papers describe the benzodiazepine fragmentation pathways after ionization [41,42] or propose corresponding fragmentation

mechanisms. The study of fragmentation pathways is important because it might allow the determination of the structure of a benzodiazepine in a biological matrix, based on the observed fragmentation pattern.

The fragmentation of protonated diazepam free of substituents has been studied [47], indicating that the most prominent peak is due to loss of CO, resulting in contraction of the seven-membered ring to a six-membered ring. It is to be expected that addition of functional groups to the diazepam molecule will result in characteristic changes of fragmentation pathways.

The main goal of the present study is the development of a mass spectral library of fragmentation pathways for a set of benzodiazepines. This library may form a starting point for predicting gas-phase fragmentations of unknown 1,4-benzodiazepines (Table 1). This library should be particularly useful in clinical and forensic analysis to perform an efficient and extensive drug screening procedure. Fragmentation spectra were studied in detail using different collision energies and declustering potentials. These energy curves were used to optimize the fragmentation voltage for each drug.

The experiments were conducted on a triple-quadrupole mass spectrometer, a prototype of the API3000 (Applied Biosystem/MDS Sciex), and a quadrupole linear ion trap mass spectrometer, a prototype of the QTRAP (Applied Biosystem/MDS Sciex).

All the 1,4-benzodiazepine samples were prepared at a concentration of 4μM, and infused in the mass spectrometer in a 50/50 water/methanol solution containing 1% acetic acid. A list of the studied benzodiazepines is given in Table 1. Nitrazepam, Norfludiazepam, Lorazepam, Triazolam and Midazolam were obtained from Cambridge Isotope Laboratories, Inc Quebec, Canada, at a concentration of 1 mg/mL in methanol. All other benzodiazepines (10 ng/μL concentration in water/methanol) were a donation of SCIEX.

In the experiments the diazepines were divided in groups according to their substitution pattern (Table 1). Group I contains the base diazepam without any substituents. The subgroup I-b contains only a substituent in position R_4. These substituents are the highly electron withdrawing Chloro or Nitro group on the benzene ring part of the azepine ring system (Desmethyl-Diazepam, Nitrazepam). The subgroup I-c contains two electron withdrawing substituents on position R_4 and R_3 for Clonazepam and on position R_4 and R_1 for Diazepam. Clonazepam has two highly electron withdrawing like Chloro and Nitro-group, while Diazepam has a Methyl substituent in

position R_1, resulting in different fragmentation pathways because the Methyl-group is a weak electron donor group.

Group II is characterized by an Hydroxy group in position R_2 (Oxazepam, Temazepam, Lorazepam). The hydroxy group is an electron withdrawing group, and easily eliminated during the fragmentation [41].

Group III contains benzodiazepines characterized by a fluorine substituent in position R_3 (Norfludiazepam, Flunitrazepam and Flurazepam) as well as various electron withdrawing substituents in positions R_1. In Norfludiazepan/ Desalkylflurazepam R_1 is a Hydrogen, and shouldn't have any particular influence. Flunitrazepam has a Methyl substituent, not so highly electron withdrawing, but also a long chain with a Nitrogen that is more highly electron withdrawing than the Methyl group, likely resulting in different fragmentation behavior.

Group IV (Alprazolam, Triazolam, and Midazolam) is structurally different from the previous groups because of the absence of the amide CO group in the ring structure. As a result, no loss of CO is possible in the fragmentation pathways. In these molecules an extra ring with one or two Nitrogens is present, therefore a loss of N_2 or NH_3 in the first fragmentation is expected.

For every benzodiazepine analyzed, the fragmentation voltage was varied between 0 – 30 eV to obtain a more detailed information about the observed fragmentation pathways. The relative abundance/intensity of the ion fragments was plotted versus the fragmentation voltage obtaining so energy resolved diagrams. These breakdown diagrams show the specific contribution of the most relevant ions to the fragmentation pattern.

Table 1. List of the studied 1,4-Benzodiazepines[1]

1,4-Benzodiazepine	R_1	R_2	R_3	R_4
		Group I-a		
Base Diazepam[2] $C_{15}H_{12}N_2O$	*H*	*H*	*H*	*H*
		Group I-b		
Desmethyl-Diazepam $C_{15}H_{11}ClN_2O$	*H*	*H*	*H*	*Cl*
Nitrazepam $C_{15}H1_5N_3O_3$	*H*	*H*	*H*	NO_2
		Group I-c		
Clonazepam $C_{15}H_{11}ClN_3O_3$	*H*	*H*	*Cl*	NO_2
Diazepam $C_{16}H_{13}ClN_2O_2$	CH_3	*H*	*H*	*Cl*
		Group II		
Oxazepam $C_{15}H_{11}ClN_2O_2$	*H*	*OH*	*H*	*Cl*
Temazepam $C_{16}H_{13}ClN_2O_2$	CH_3	*OH*	*H*	*Cl*
Lorazepam $C_{15}H_{10}Cl_2N_2O_2$	*H*	*OH*	*Cl*	*Cl*
		Group III		
Flurazepam $C_{21}H_{23}ClFN_3O$	$CH_2CH_2N(CH_2CH_3)_2$	*H*	*F*	*Cl*
Flunitrazepam $C_{16}H_{12}FN_3O$	CH_3	*H*	*F*	NO_2
Norfludiazepam $C_{15}H_{13}FN_2O$	*H*	*H*	*F*	*Cl*
		Group IV		
Alprazolam* $C_{17}H_{13}ClN_4$	$(C(CH_3)NN)$	*H*	*H*	*Cl*
Triazolam* $C_{17}H_{12}Cl_2N_4$	$(C(CH_3)NN)$	*H*	*Cl*	*Cl*
Midazolam* $C_{18}H_{13}ClFN_3$	$(C(CH_3)NCH)$	*H*	*F*	*Cl*
		Group V		
Bromazepam[2] $C_{14}H_{10}BrN_3O$	*H*	*H*	*(N)*	*Br*

[1] R_1, R_2, R_3 and R_4 on the 1,4-benzodiazepam nucleus are specified in Fig.1.
[2] Results obtained by Joey B.Y. Cheng.
* no CO group.

4.1 Decomposition of Group I

Desmethyldiazepam – Nitrazepam (Group I-b) and Diazepam - Clonazepam (Group I-c) are two drugs with only a single difference in the substituents, so the fragmentation pathway should be very similar between the two molecules.

4.2 Group I-b: Desmethyldiazepam

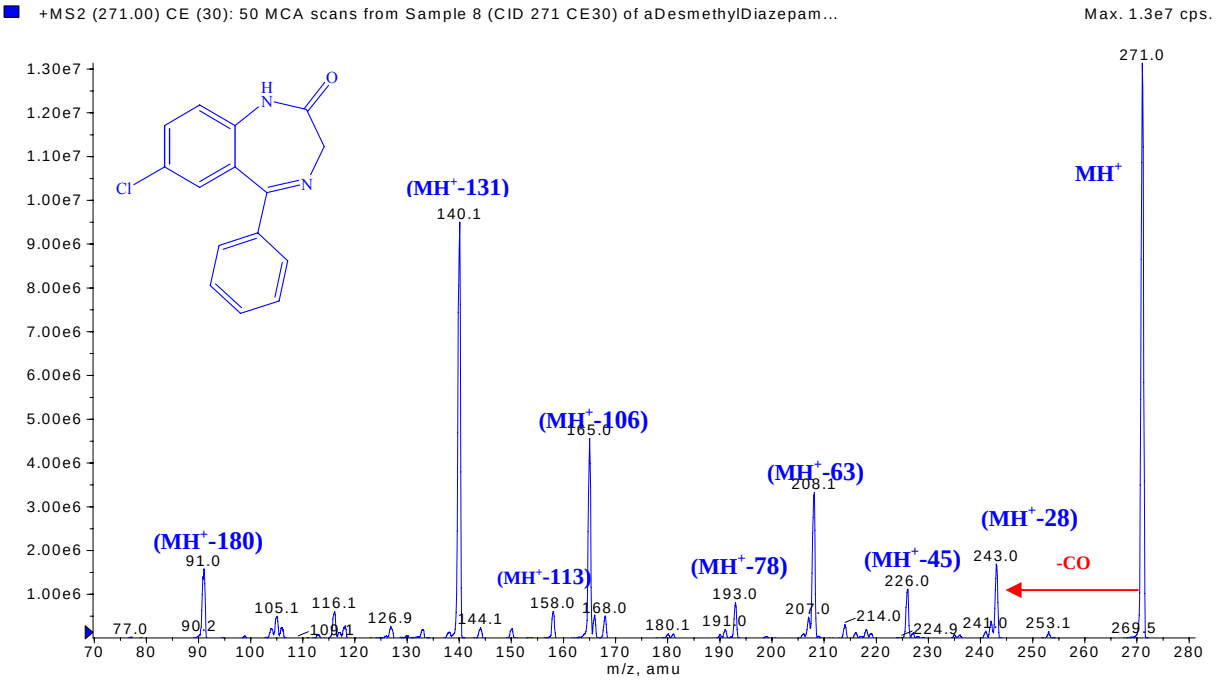

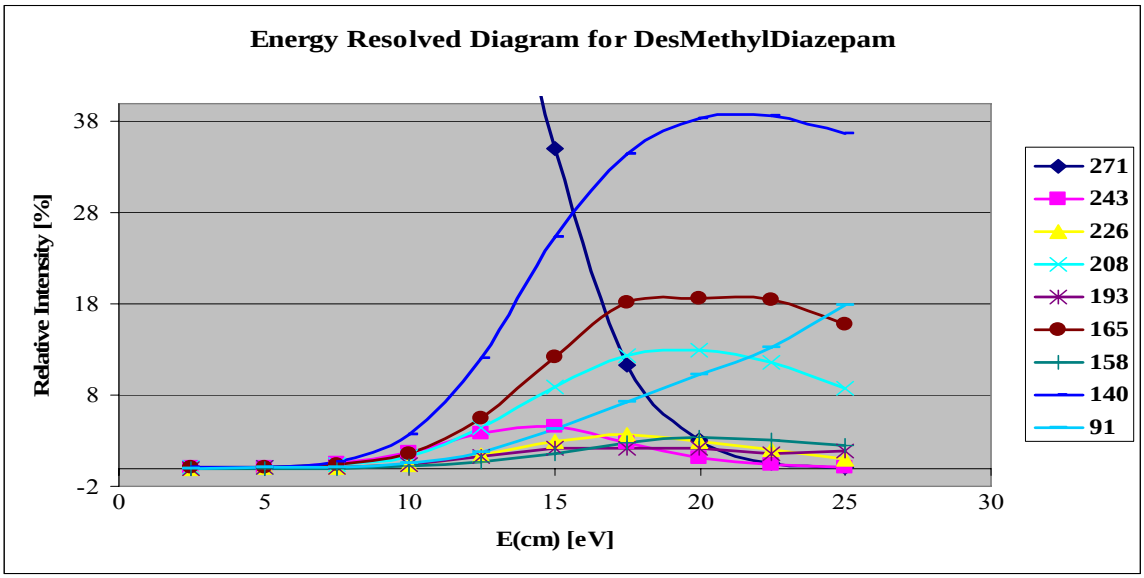

Fragmentation Pathway Proposal for DesMethylDiazepam

1)

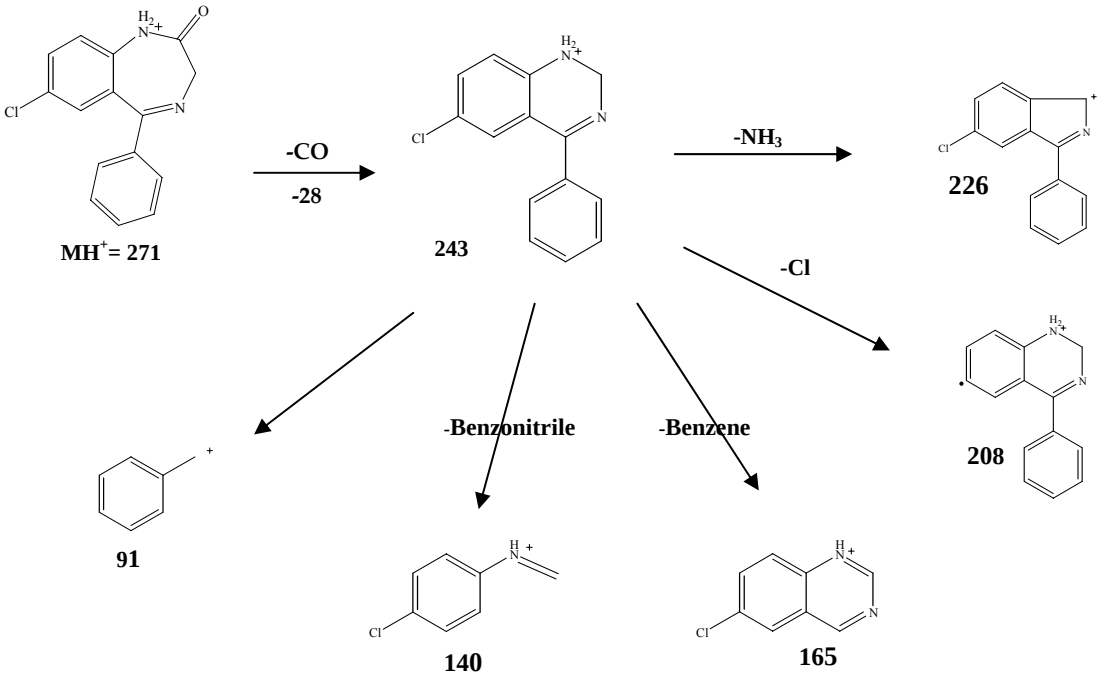

2)

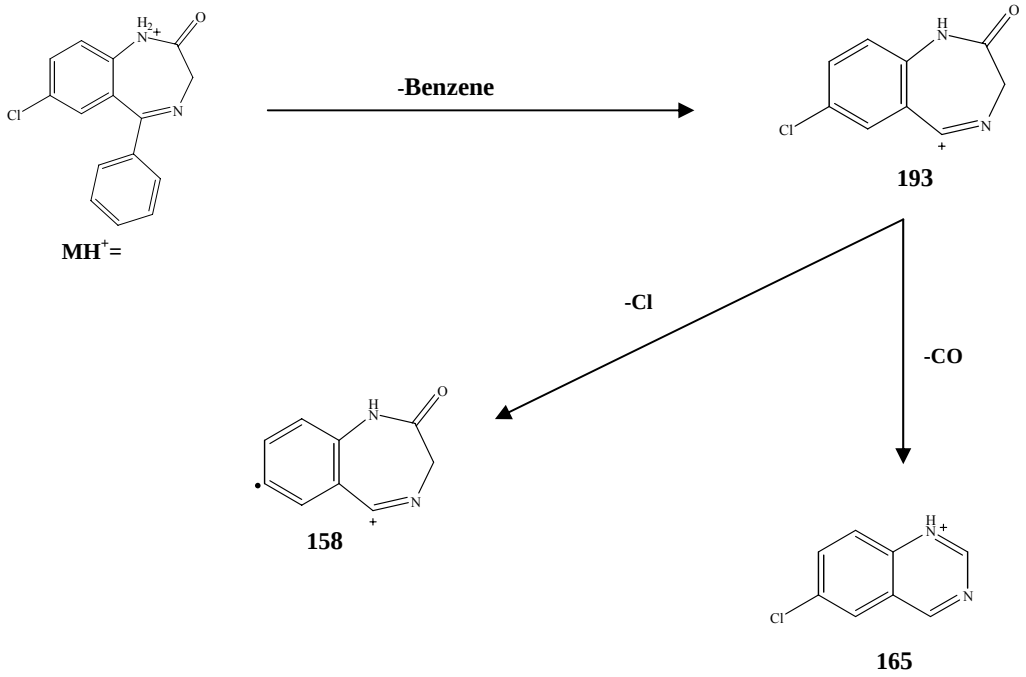

Desmethyldiazepam

After electrospray ionization, the collisional activation of the protonated molecule results in primary loss of CO with rearrangement of the diazepine ring to a 1,2-dihydro-pyrimidine ring. The resulting fragment in turn decomposes into five main fragments which constitute the greater part of the fragmentation. The loss of a NH_3 group causes a further rearrangement of the 1,2-dihydro-pyrimidine ring to a pyrrole ring $[MH - CO - NH_3]^+$, whereas a prominent fragment is due to the loss of a benzonitrile group $[MH - CO - PhCN]^+$. Other fragments are due to the loss of a chorine atom $[MH - CO - Cl]^+$ and of the benzene ring $[MH - CO - Ph]^+$. The last main fragment is the benzyl group. A competitive fragmentation pathway first assumes loss of the benzene group from the protonated molecule which in turn gives two main fragments due to the loss of Cl $[MH - Ph - Cl]^+$ and CO $[MH - Ph - CO]^+$. The energy resolved plots show that the curves of the fragments obtained from the loss of benzonitrile, benzene and chlorine groups, after the CO loss, increase with the fragmentation energy until a plateau is reached at around 20 eV. In contrast, the formation of the other main fragments seems to be unaffected by the fragmentation energy. The benzene group is the only fragment which shows an exponential growth when the energy increases.

4.3 Group I-b: Nitrazepam

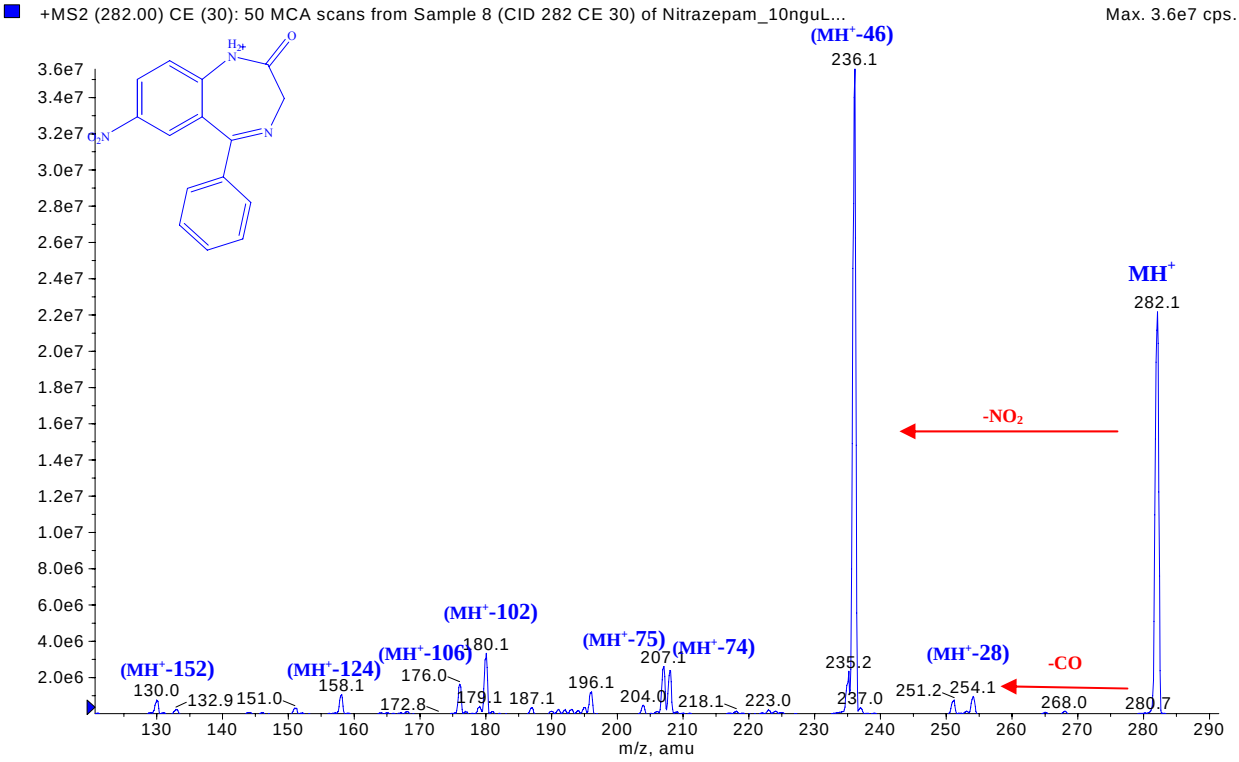

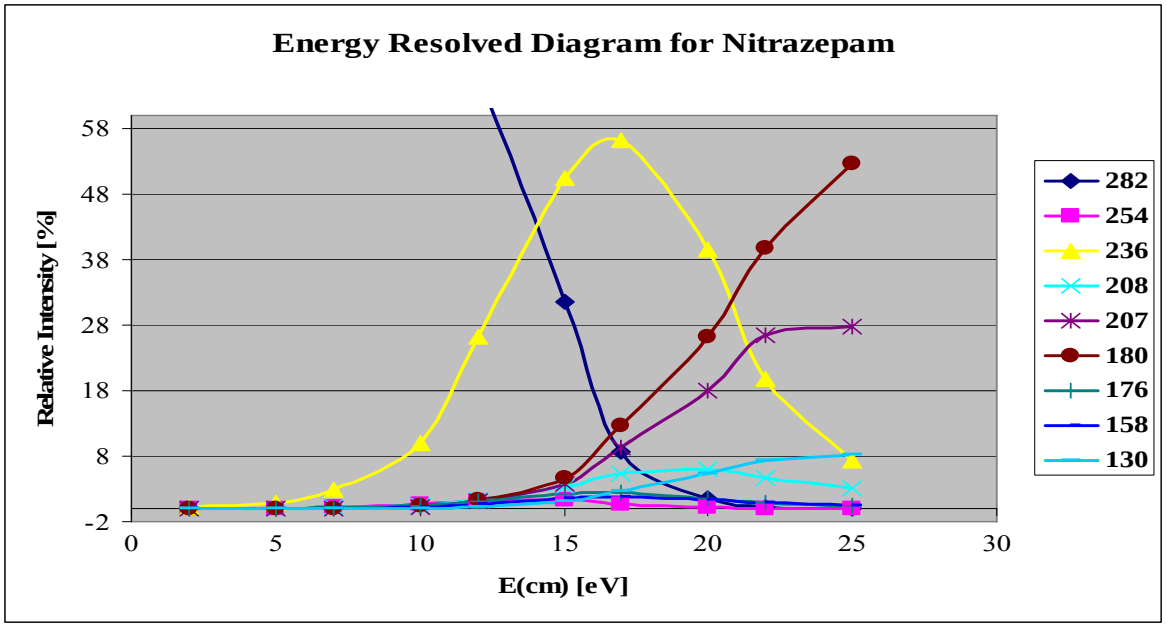

Fragmentation Pathway Proposal for Nitrazepam

1)

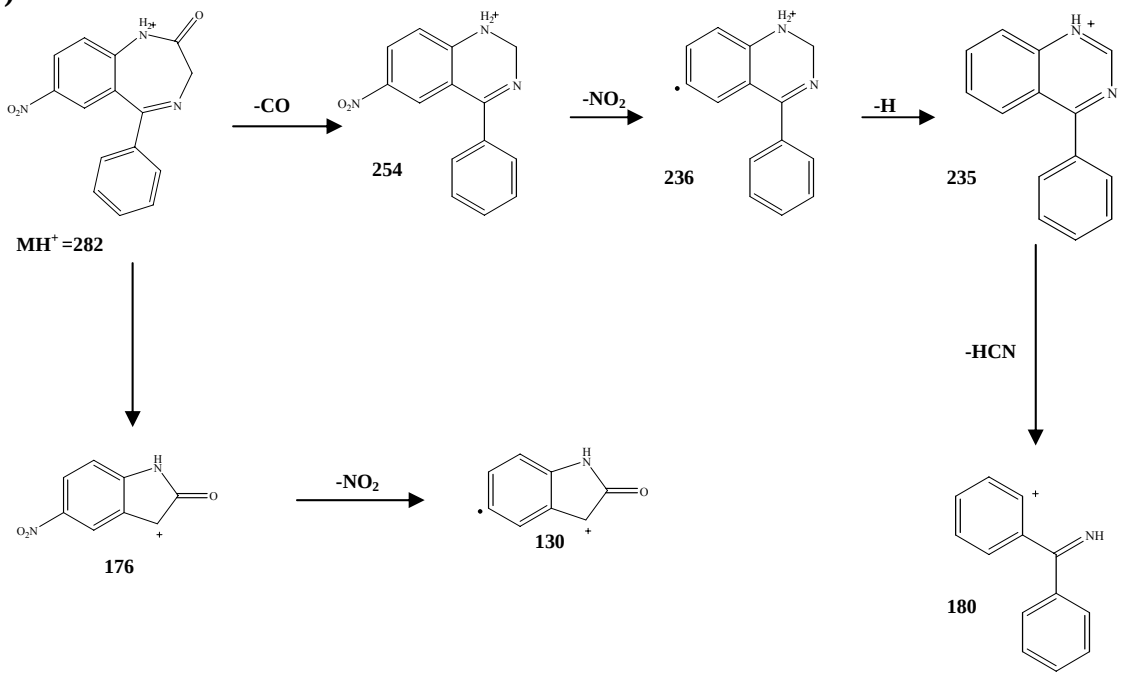

2)

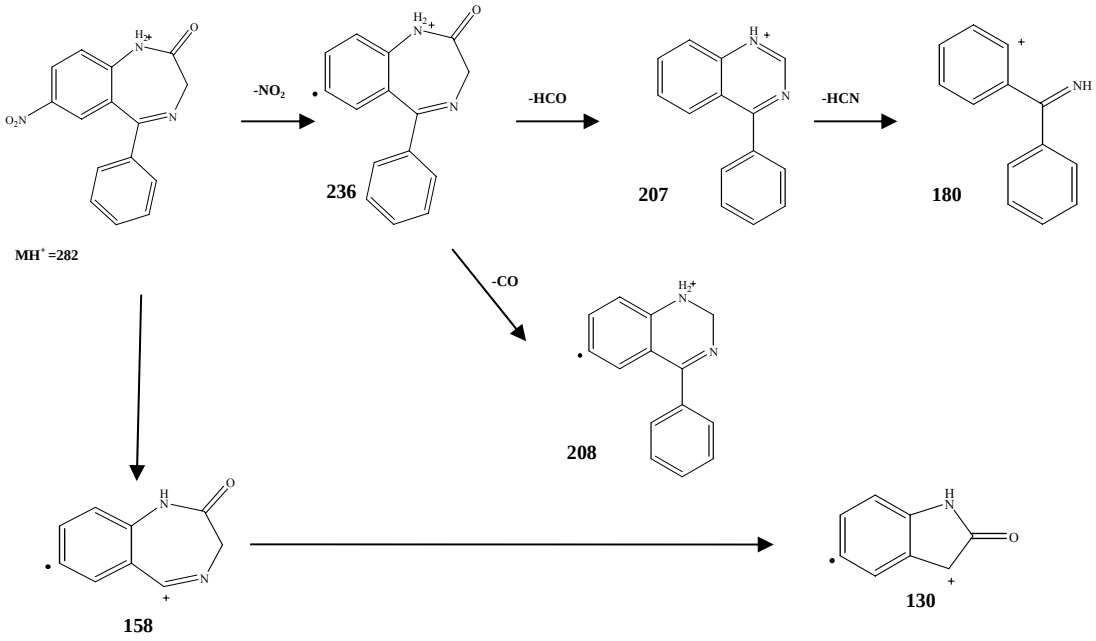

Nitrazepam

Collisional activation of the protonated molecule, as generated by electrospray ionization, induces a primary loss of CO with the rearrangement of the diazepine ring to a 1,2-dihydro-pyrimidine ring. The resulting fragment in turn decomposes into a second fragment with the loss of NO_2 and the formation of $[MH - CO - NO_2]^+$. This fragment can easily lose an Hydrogen atom, followed by HCN $[MH - CO - NO_2 - H - HCN]^+$. A further fragment is due to the loss of a benzonitrile group $[MH - PhCN]^+$, that fragments by losing NO_2 $[MH - PhCN - NO_2]^+$. Other fragments are due to the loss of the benzene ring $[MH - Ph]^+$, and a subsequent loss of CO $[MH - Ph - CO]^+$. An alternative fragmentation pathway assumes in a first step loss of the NO_2 group from the protonated molecule which in turn yields two main fragments due to the loss of CO $[MH - NO_2 - CO]^+$ and HCO $[MH - NO_2 - HCO]^+$. The $[MH - NO_2 - HCO]^+$ fragment subsequently can eject HCN to give $[MH - NO_2 - HCO - HCN]^+$. The energy resolved plots show that the curves of the fragments obtained from the loss of NO_2, CO, H and HCN, after NO_2 and CO loss, increase with the fragmentation energy. In contrast, the formation of the other main fragments seem to be unaffected by the fragmentation energy.

4.4 Group I-c: Diazepam

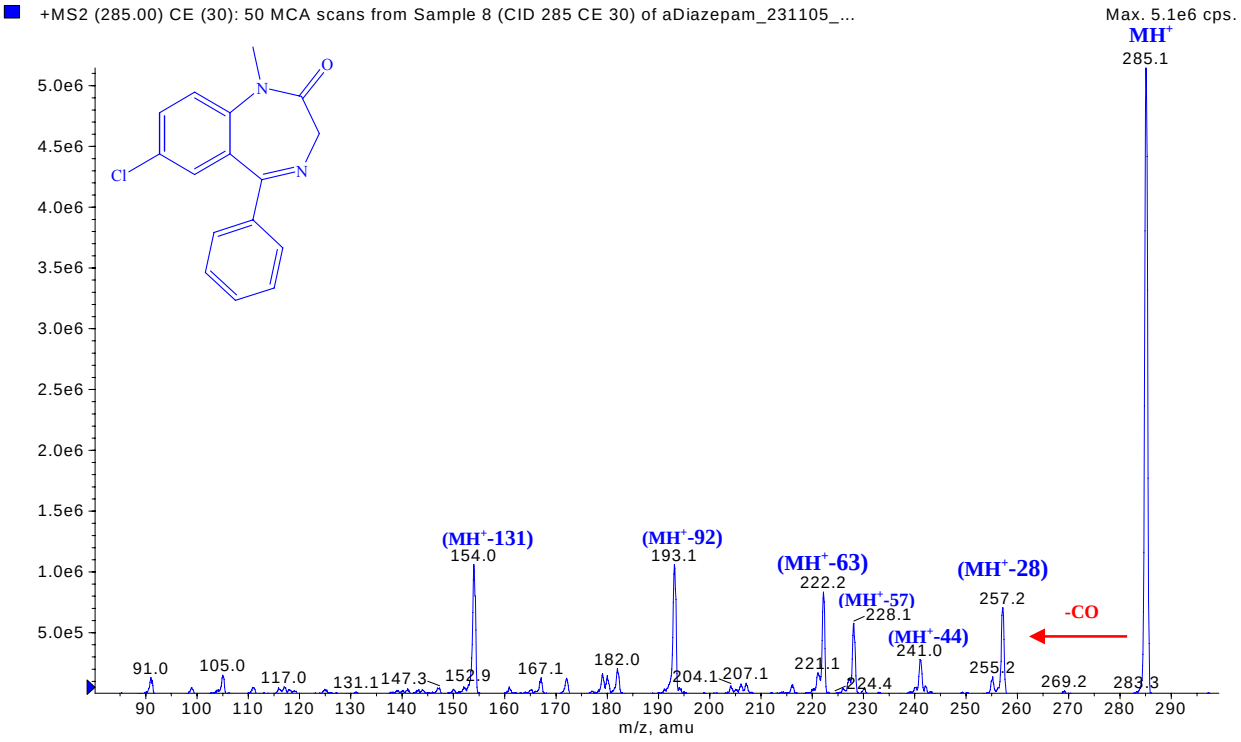

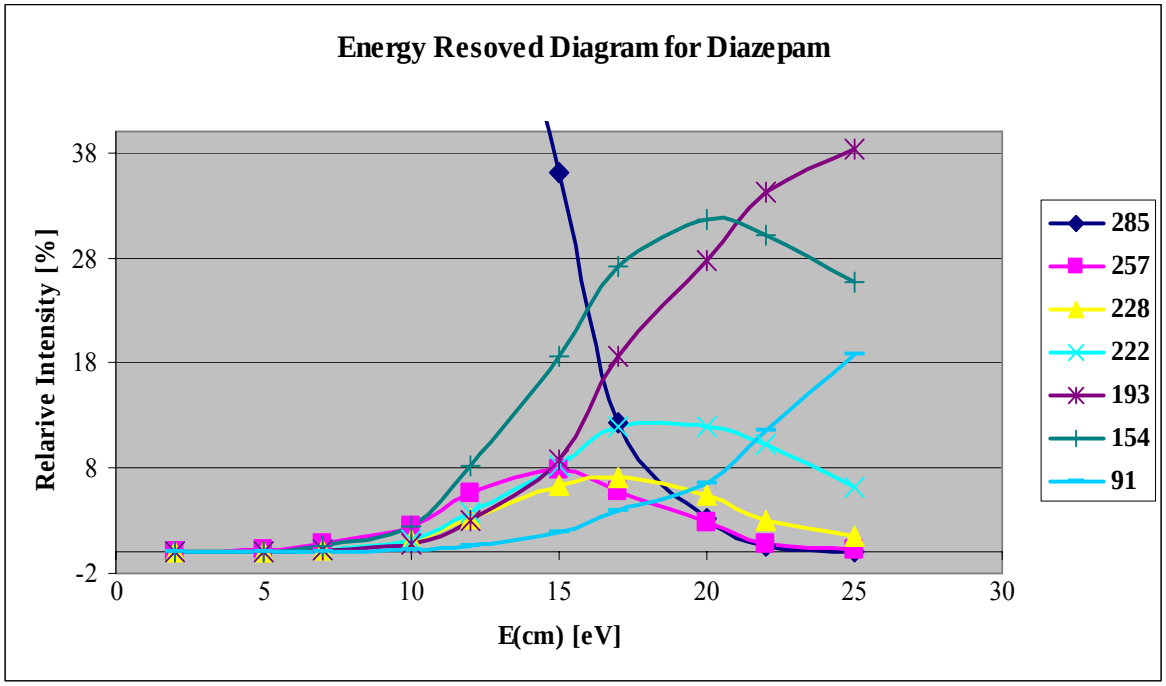

Fragmentation Pathway Proposal for Diazepam

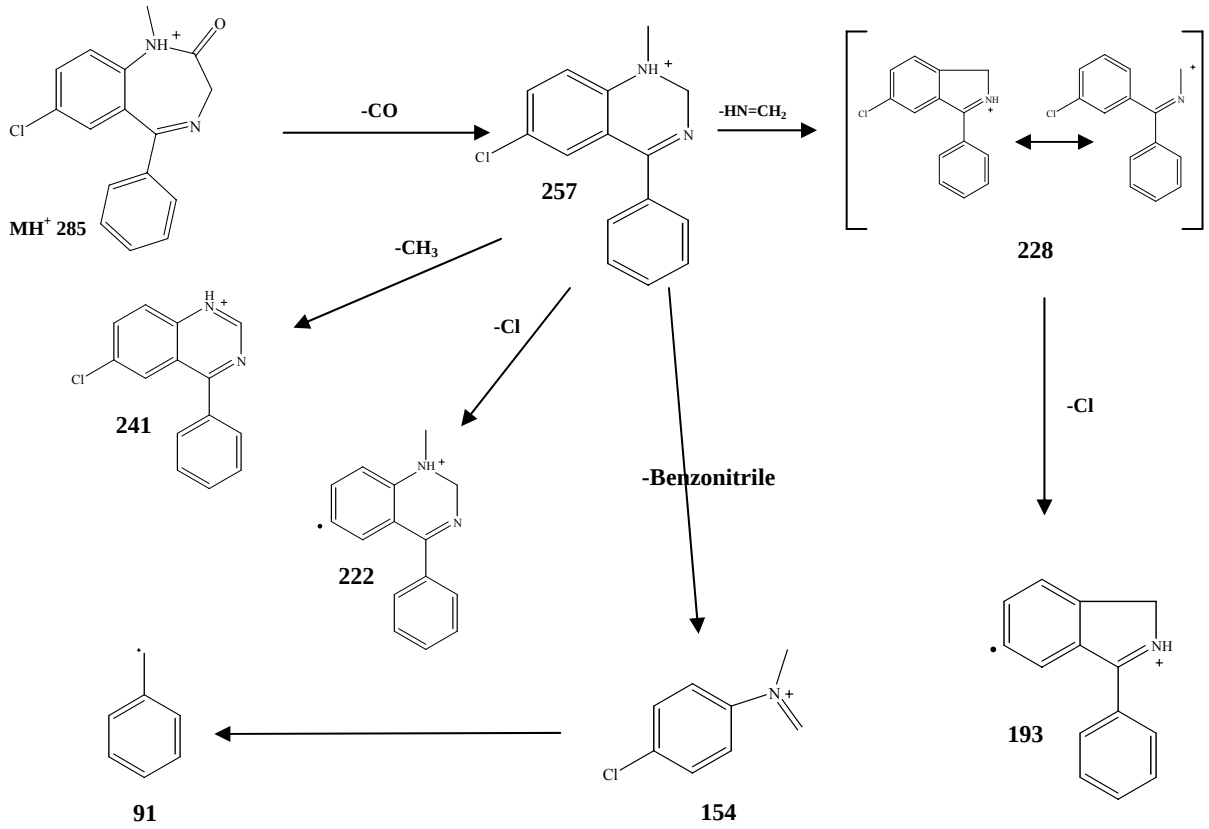

Diazepam

With features analogous of the other compounds, the collision step of the protonated molecule induces a primary loss of CO with rearrangement of the diazepine ring to a 1,2-dihydro-pyrimidine ring. The resulting fragment in turn dissociates into four main fragments which constitute the greater part of the fragmentation. The loss of a $NH{=}CH_2$ group causes a further rearrangement of the 1,2-dihydro-pyrimidine ring to a pyrrole ring $[MH - CO - NH{=}CH_2]^+$, followed by loss of chlorine $[MH - CO - NN{=}CH_2 - Cl]^+$. In addition a pronounced fragment, due to the loss of a benzonitrile group $[MH - CO - PhCN]^+$, is present. Other fragments are due to the loss of a chorine atom $[MH - CO - Cl]^+$ a methyl group $[MH - CO - CH_3]^+$, and the toluene group. The energy resolved plots show that the curves of the fragments obtained through loss of the benzonitrile and chlorine groups (after the CO loss) increase with the fragmentation energy. In contrast, the formation of the other main fragments seem to be unaffected by the fragmentation energy. The toluene group is the only fragment which shows exponential growth of intentsity when the collision energy increases.

4.5 Group 1-c: Clonazepam

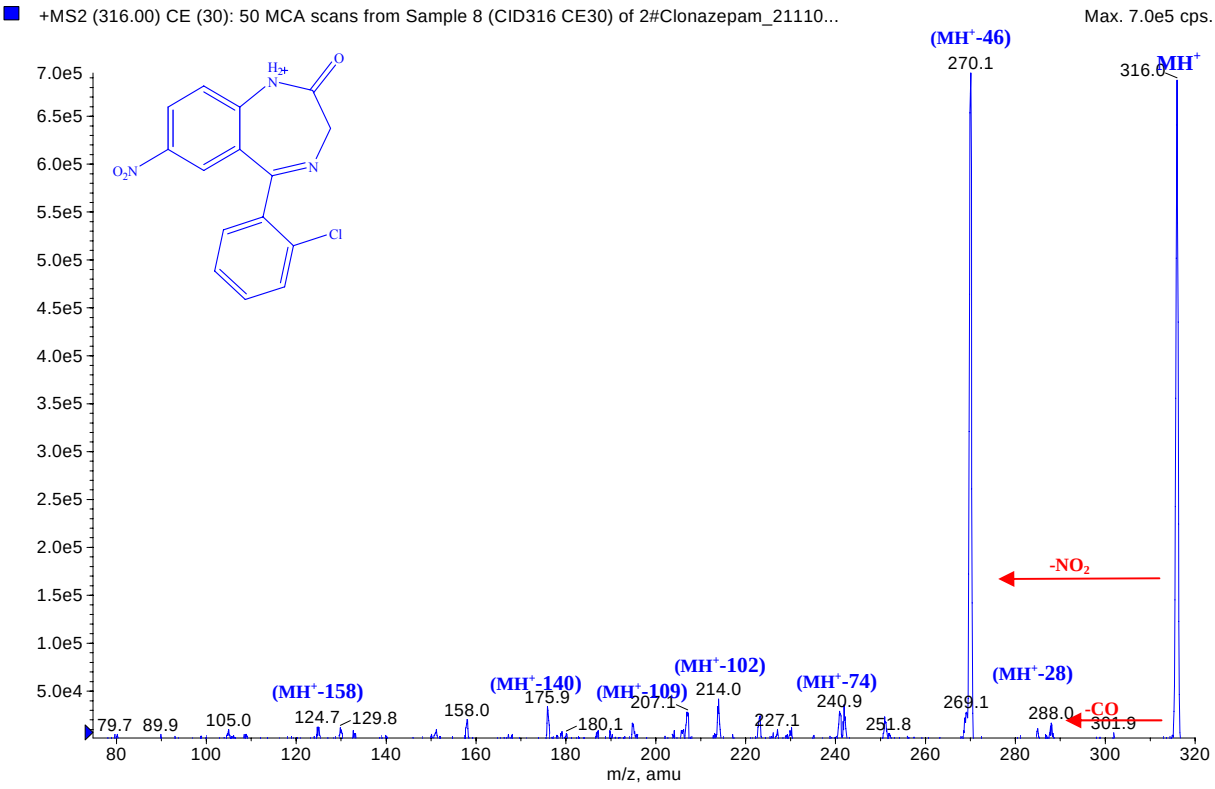

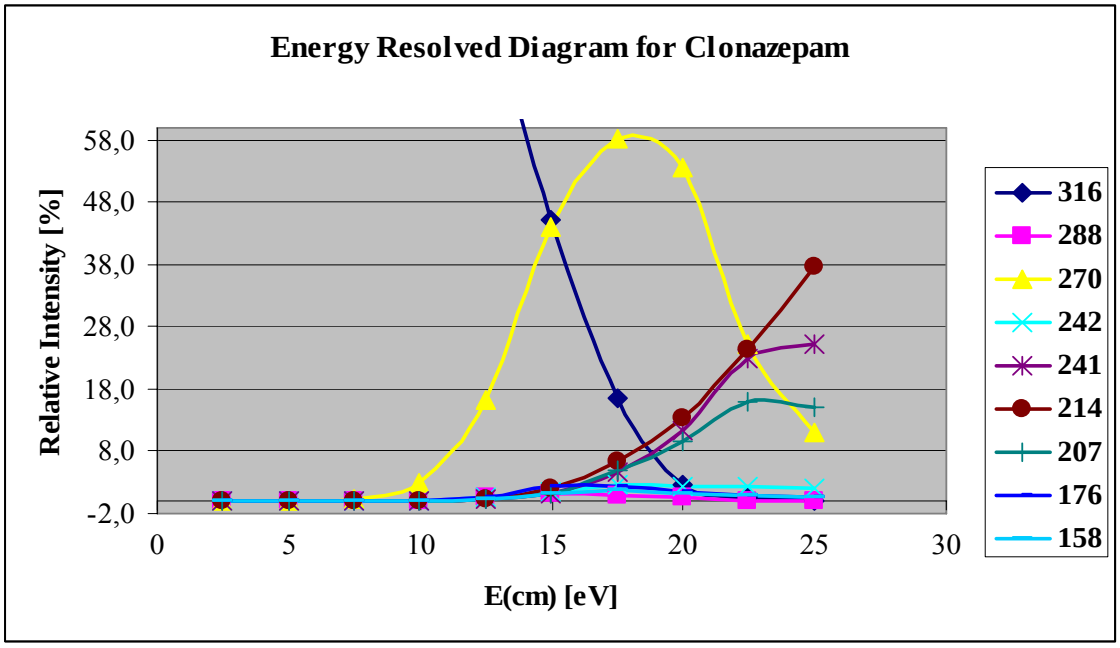

Fragmentation Pathway Proposal for Clonazepam

1)

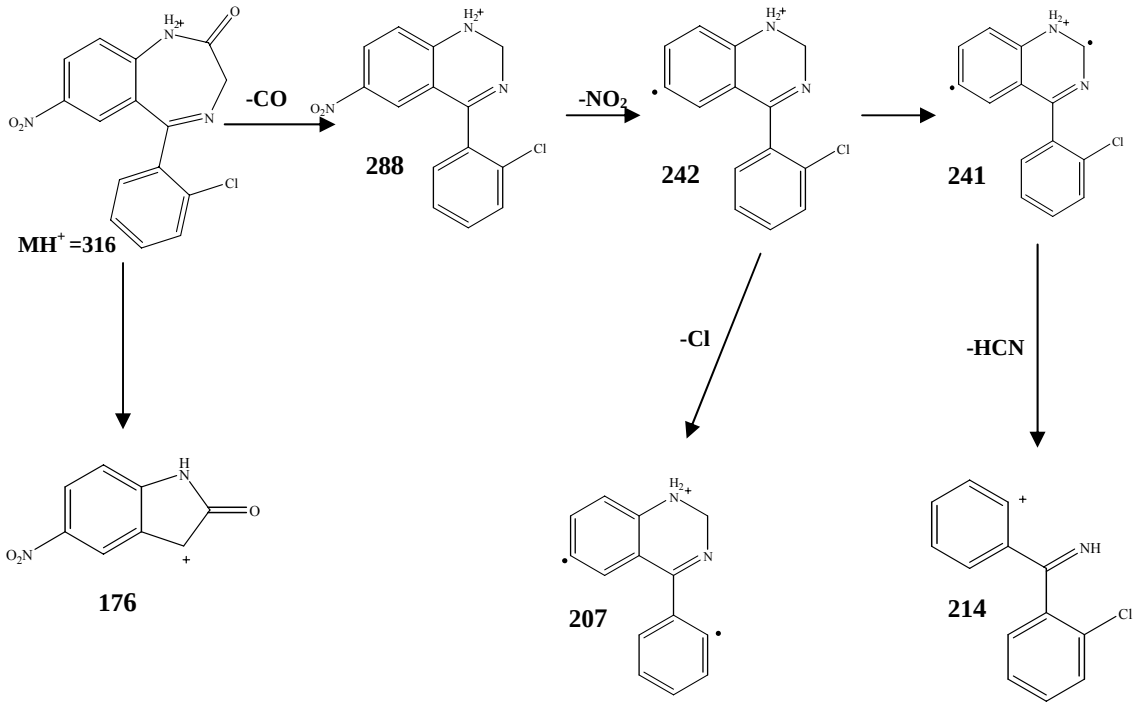

2)

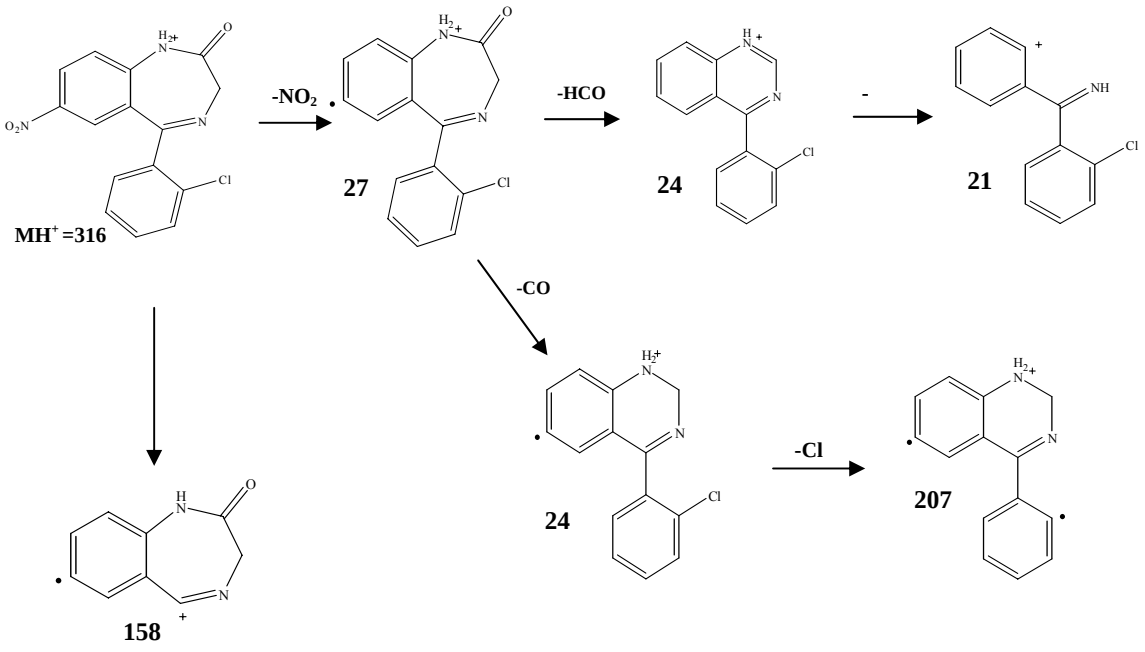

Clonazepam

After electrospray ionization, the collisional activation of the protonated molecule induces primary loss of CO followed by rearrangement of the diazepine ring to a 1,2-dihydro-pyrimidine ring. The resulting fragment in turn fragments by loss of NO_2 and the formation of $[MH - CO - NO_2]^+$. This fragment can easily lose an Hydrogen and HCN $[MH - CO - NO_2 - H - HCN]^+$. Loss of the chlorine $[MH - CO - NO_2 - Cl]^+$.competes with loss of HCN. A fragment due to the loss of a benzonitrile group $[MH - PhCN]^+$ is present as well, together with a fragment due to loss of the benzene ring $[MH - Ph]^+$. A competitive fragmentation pathway assumes a first loss of the NO_2 group from the protonated molecule which in turn yields two main fragments due to the loss of CO $[MH - NO_2 - CO]^+$ and HCO $[MH - NO_2 - HCO]^+$. In scheme 2 loss of HCN $[MH - NO_2 - HCO - HCN]^+$ from structure 24 and loss of chlorine $[MH - NO_2 - CO - Cl]^+$ from structure 24 are shown. The energy resolved plots show that the curves of the fragments obtained by loss of NO_2, CO, H and HCN, or the loss of NO_2, CO and chlorine after the NO_2 and CO loss, increase with the fragmentation energy. In contrast, the formation of the other main fragments seem to be unaffected by the fragmentation energy.

4.6 Group II

4.7 Group II: Oxazepam

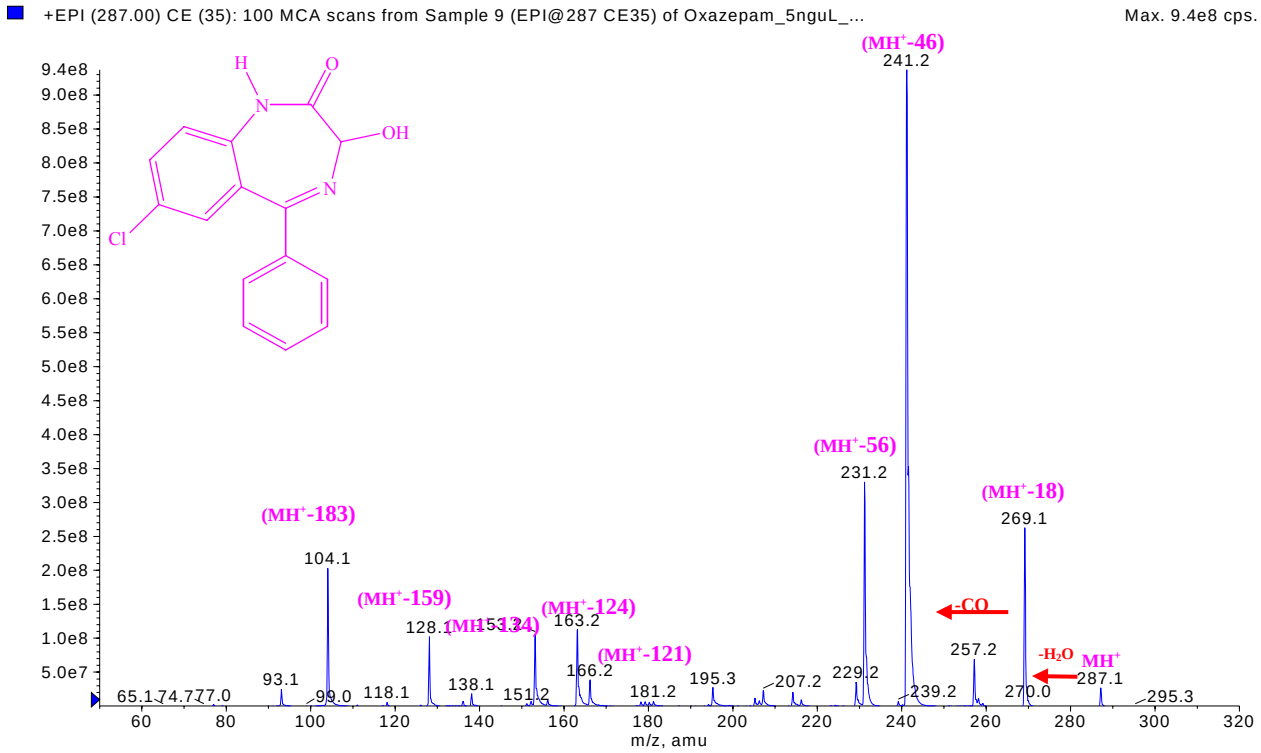

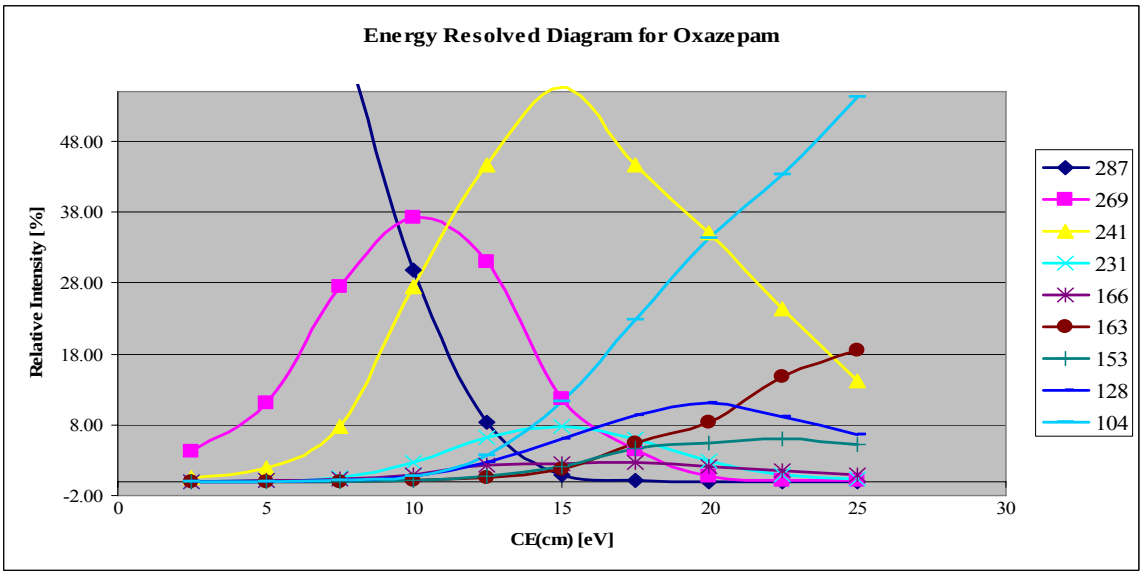

Fragmentation Pathway Proposal for Oxazepam

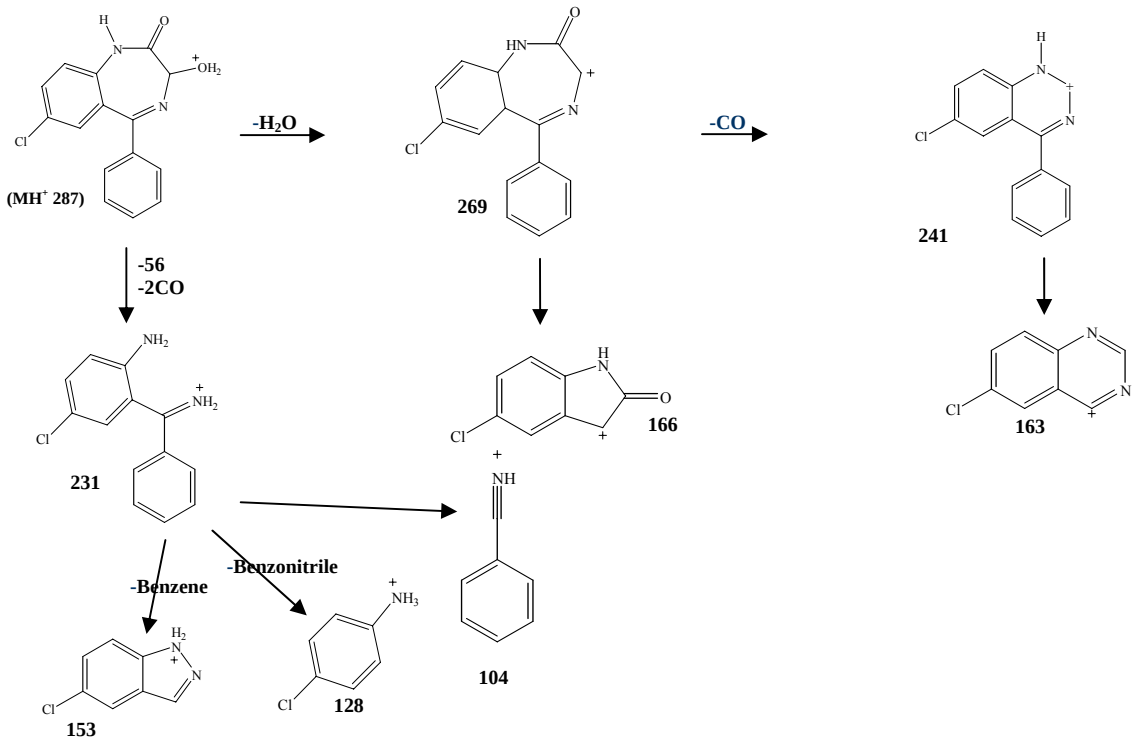

Oxazepam

After electrospray ionization, the collisional activation of the protonated molecule results in primary loss of H_2O followed by loss of CO under rearrangement of the diazepine ring to a 1,2-dihydro-pyrimidine ring. After the loss of water, the loss of benzonitrile $[MH - H_2O - PhCN]^+$ can take place. The combined loss of water and CO can initiate the loss of benzene $[MH -H_2O - CO - Ph]^+$. A competitive fragmentation pathway assumes a first loss of two molecules of CO with the resulting fragment in turn yielding two main fragments due to the loss of benzene $[MH -CO -CO - Ph]^+$ and benzonitrile $[MH -CO -CO -PhCN]^+$ due to proton transfer. The energy resolved plots show that the curves of the fragments obtained from the loss of benzonitrile and benzene after the H_2O and CO loss, increases with the fragmentation energy. In contrast, the formation of the other main fragments seem to unaffected by the fragmentation energy. The benzonitrile group is the only fragment which shows an exponential growth when the collision energy increases.

4.8 Group II: Temazepam

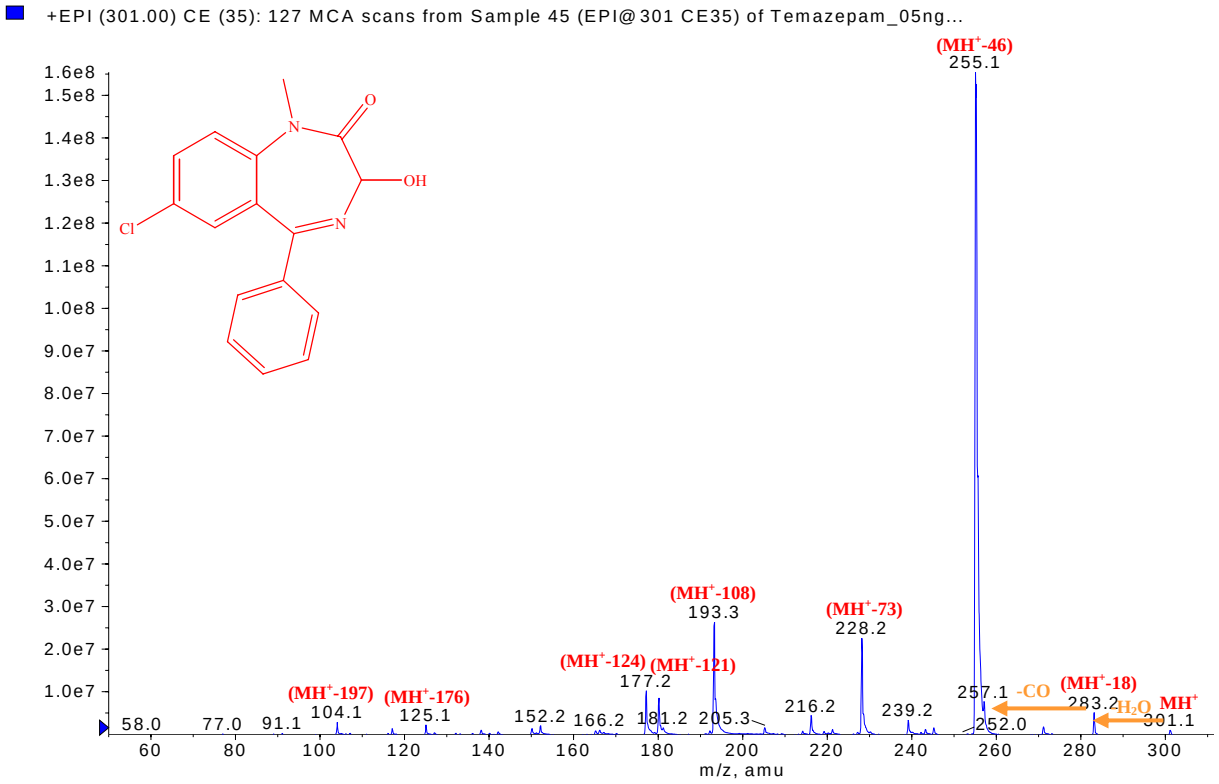

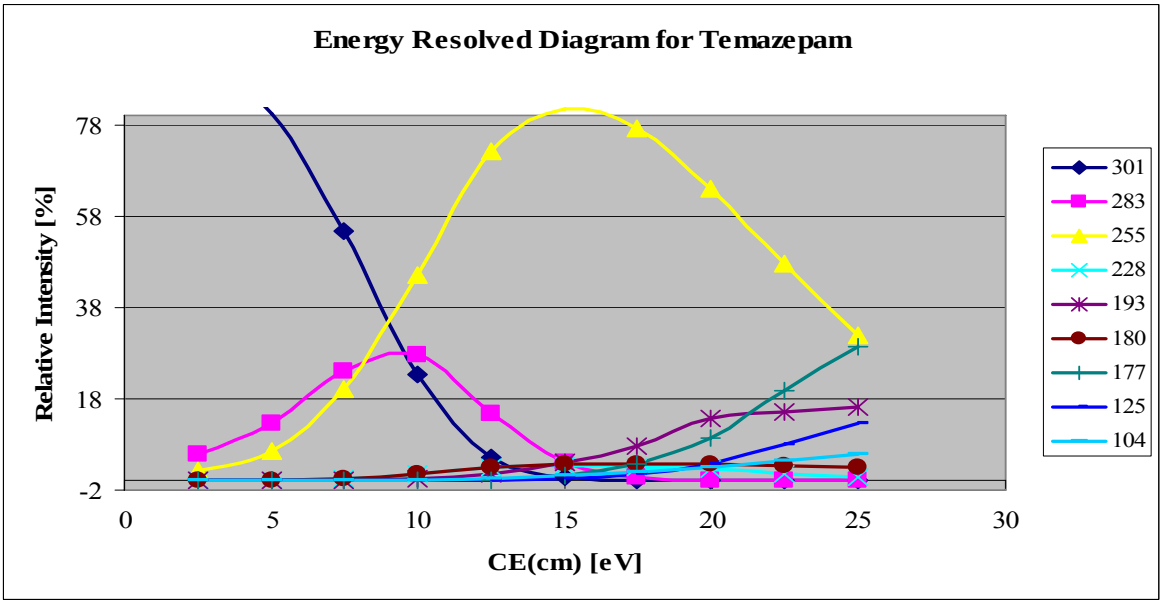

Fragmentation Pathway Proposal for Temazepam

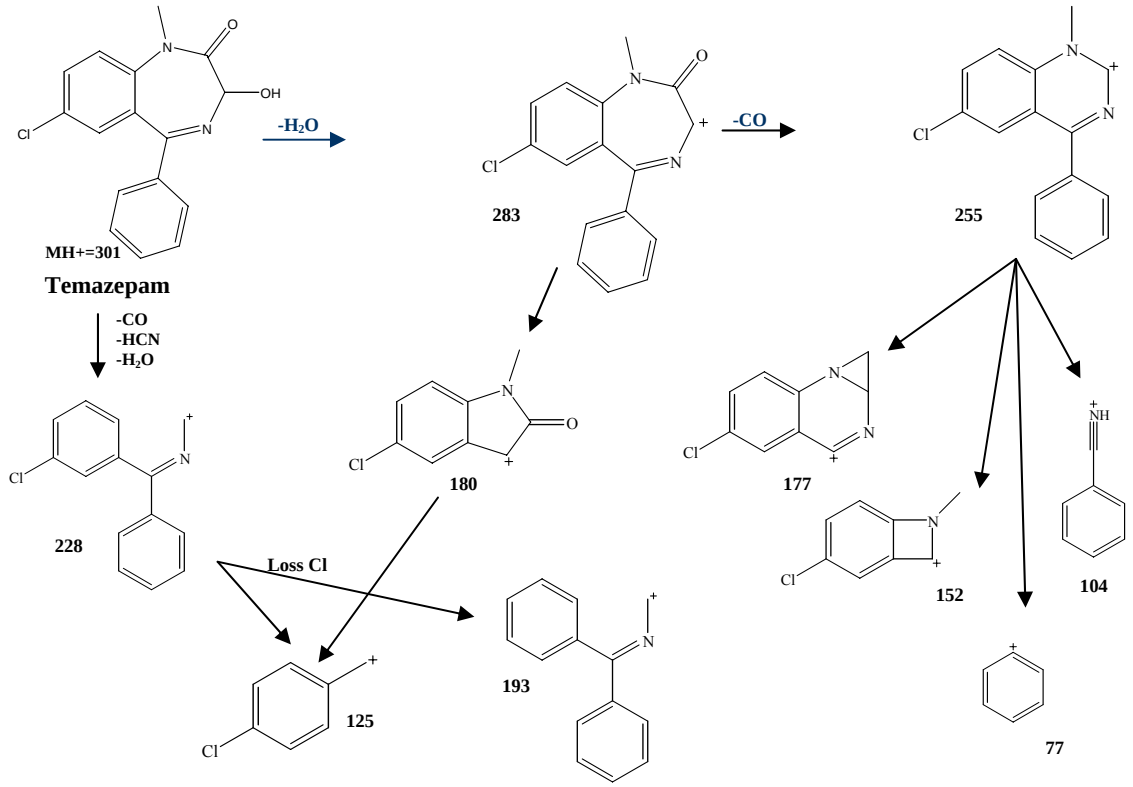

Temazepam

After electrospray ionization, the collisional activation of the protonated molecule induces loss of H_2O followed by loss of CO with the rearrangement of the diazepine ring to a 1,2-dihydro-pyrimidine ring. After the loss of water, benzonitrile $[MH - H_2O - PhCN]^+$ can be lost. After the loss of water and CO, loss of Benzene $[MH -H_2O - CO - Ph]^+$ and benzonitrile $[MH -H_2O - CO - PhCN]^+$ are observed A competitive fragmentation pathway assumes a first loss of CO, HCN and H_2O which in turn gives two main fragments due to the loss of chlorine $[MH -CO -HCN -H_2O - Cl]^+$ and benzonitrile $[MH -CO -HCN -H_2O -PhCN]^+$. The energy resolved plots show that the curves of the fragments obtained from the loss of benzene, after H_2O and CO loss, increase with the fragmentation energy, as do the curves obtained from the loss of chlorine, CO, HCN, and H_2O. In contrast, the formation of the other fragments seem to be unaffected by the fragmentation energy.

4.9 Group II: Lorazepam

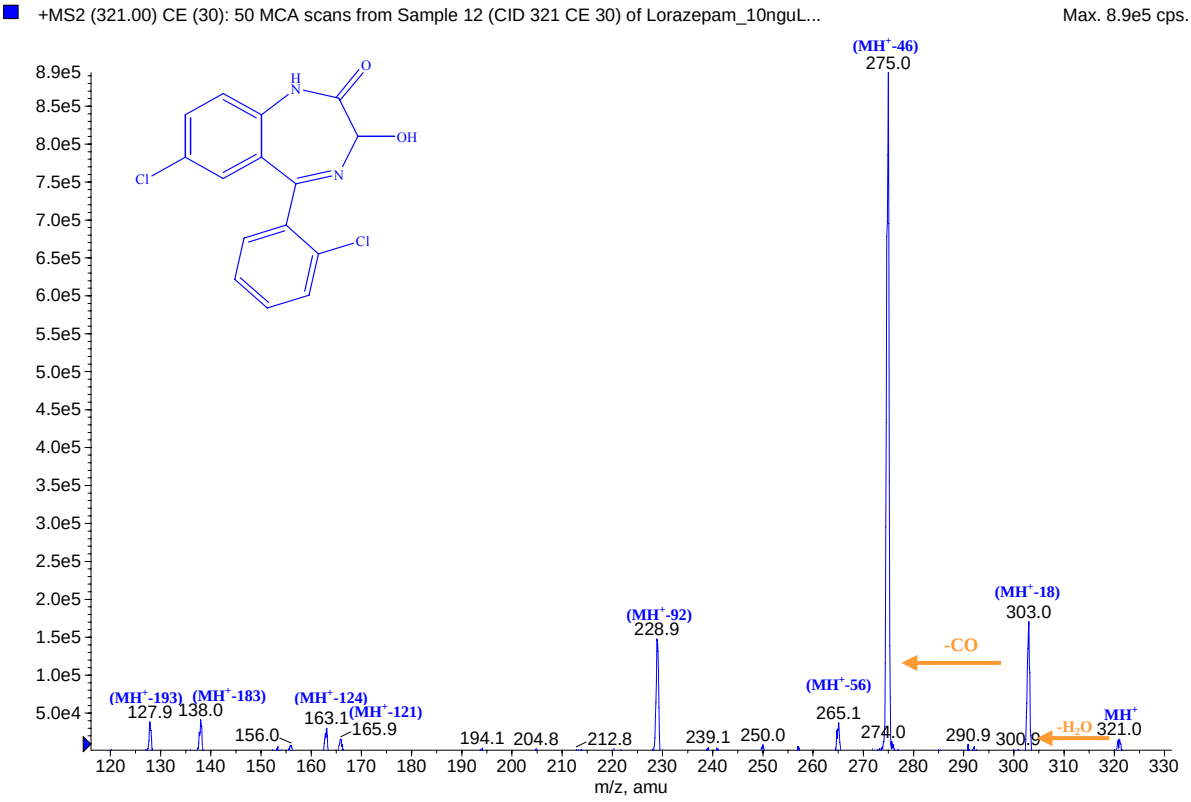

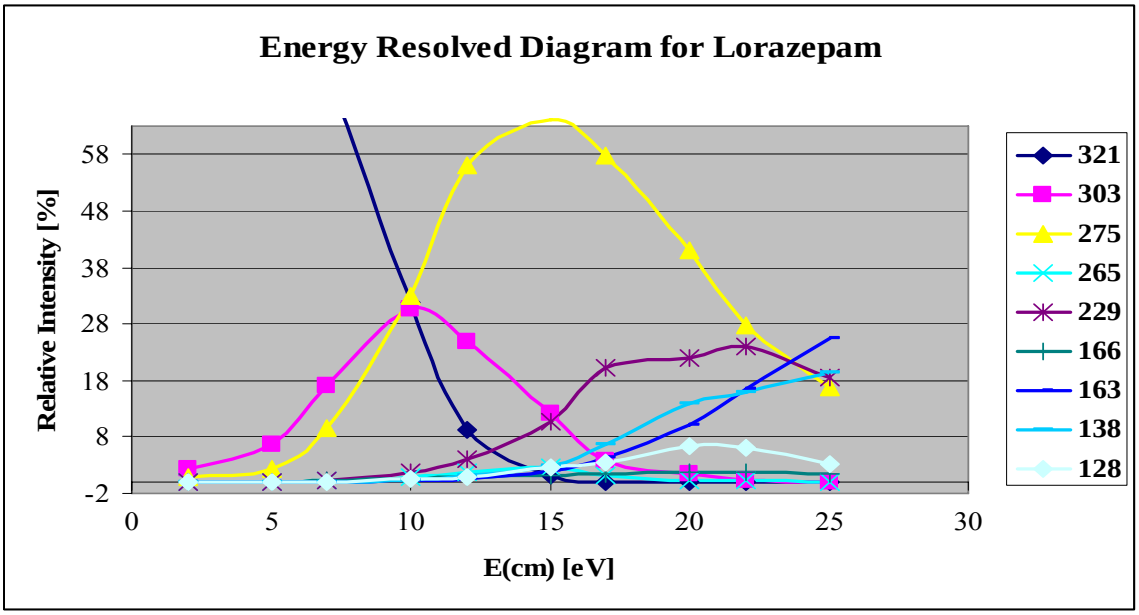

Fragmentation Pathway Hypothesis for Lorazepam

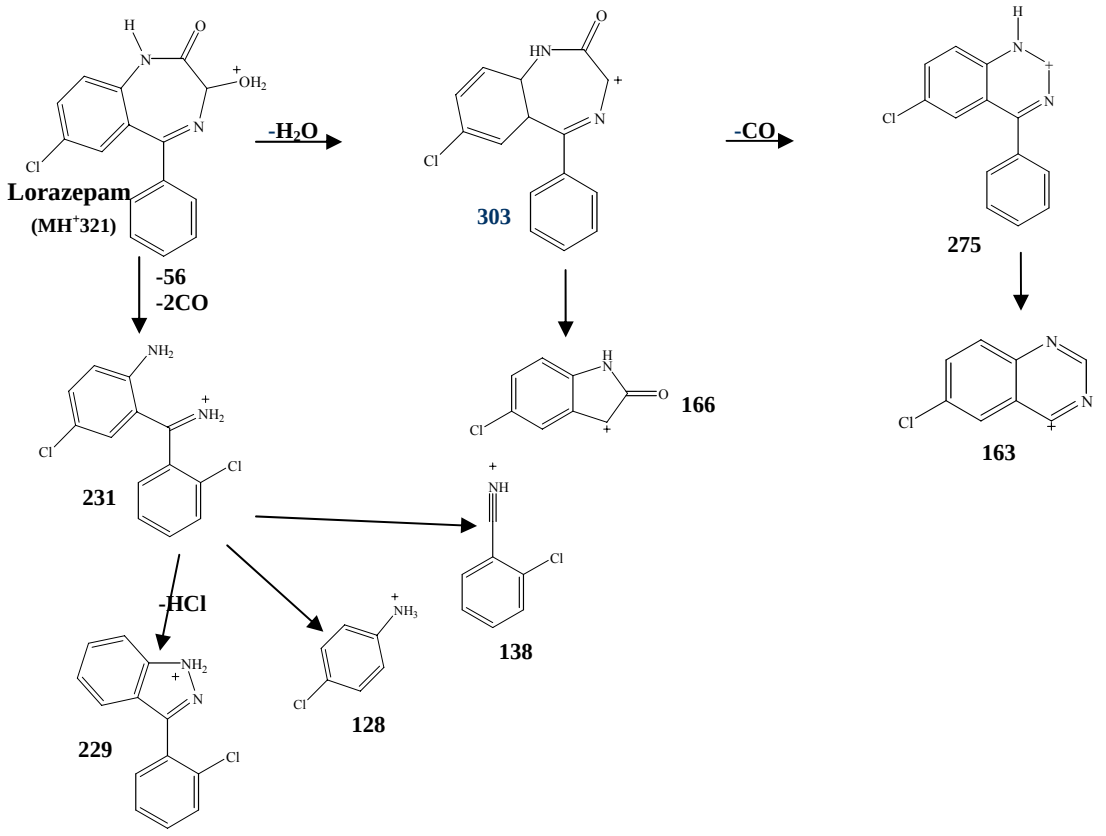

Lorazepam

After electrospray ionization, the collisional activation of the protonated molecule induces a primary loss of H_2O followed by a loss of CO with the rearrangement of the diazepine ring to a 1,2-dihydro-pyrimidine ring. Starting with loss of water, the loss of benzonitrile $[MH - H_2O - PhCN]^+$ is shown, while after the loss of water and CO loss of Benzene $[MH - H_2O - CO - Ph]^+$ can take place. A competitive fragmentation pathway assumes a first loss of two molecules of CO which in turn gives two main fragments due to the loss of Chlorine $[MH - CO - CO - Cl]^+$ and benzonitrile $[MH - CO - CO - PhCN]^+$. The energy resolved plots show that the curves of the fragments obtained from the loss of benzene, after H_2O and CO loss, increase with the fragmentation energy. In contrast, the formation of the other main fragments are unaffected by the fragmentation energy. The benzonitrile group is the only fragment which shows an exponential growth when the energy increases.

4.10 Group III

4.11 Group III: Norfludiazepam (Desalkylflurazepam)

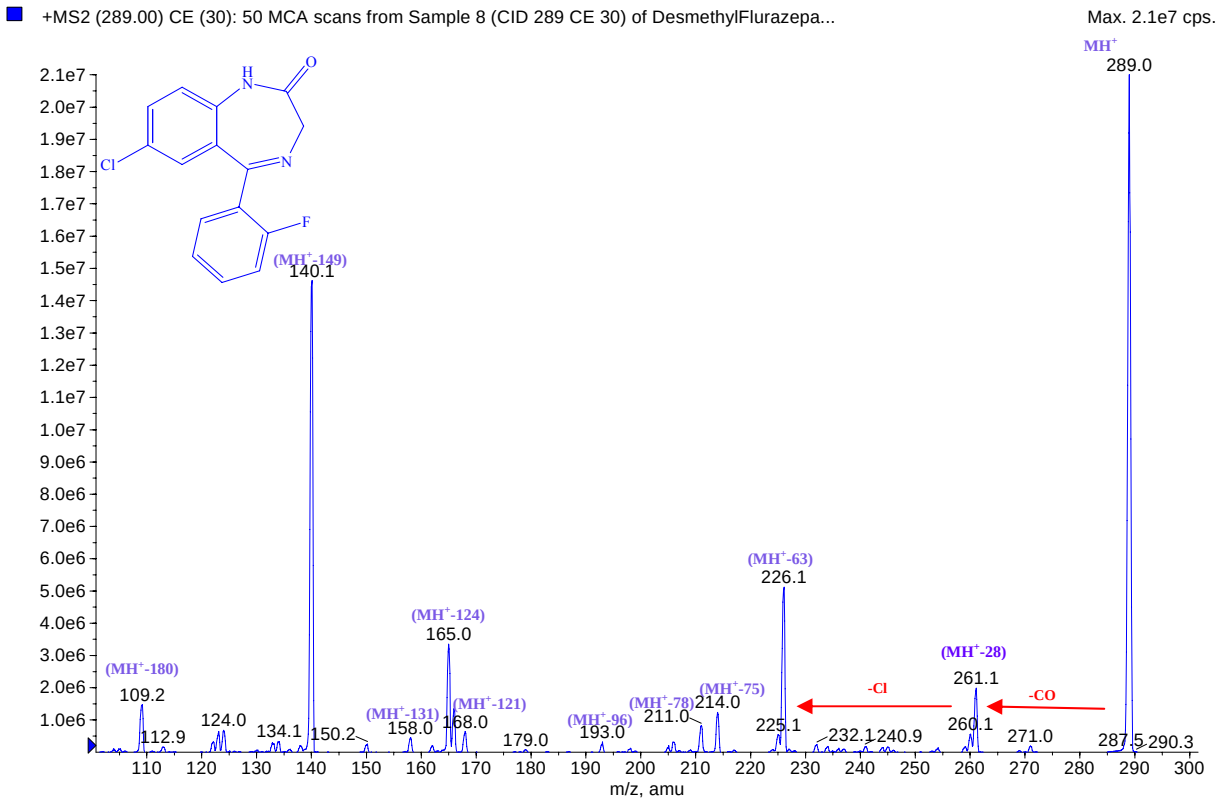

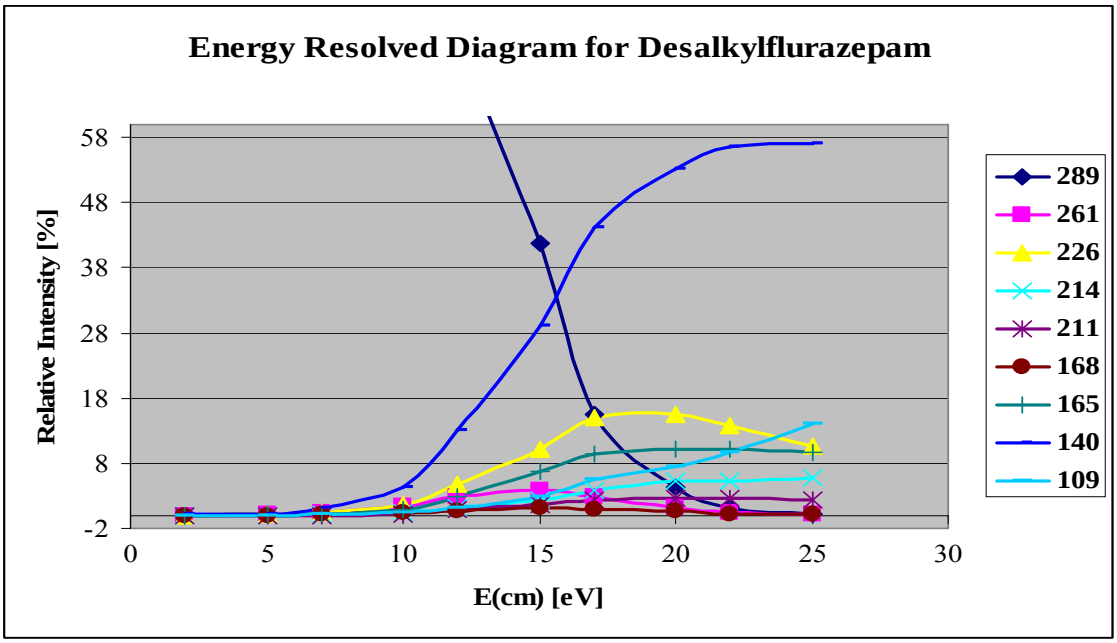

Fragmentation Pathway Proposal for DesalkylFlurazepam

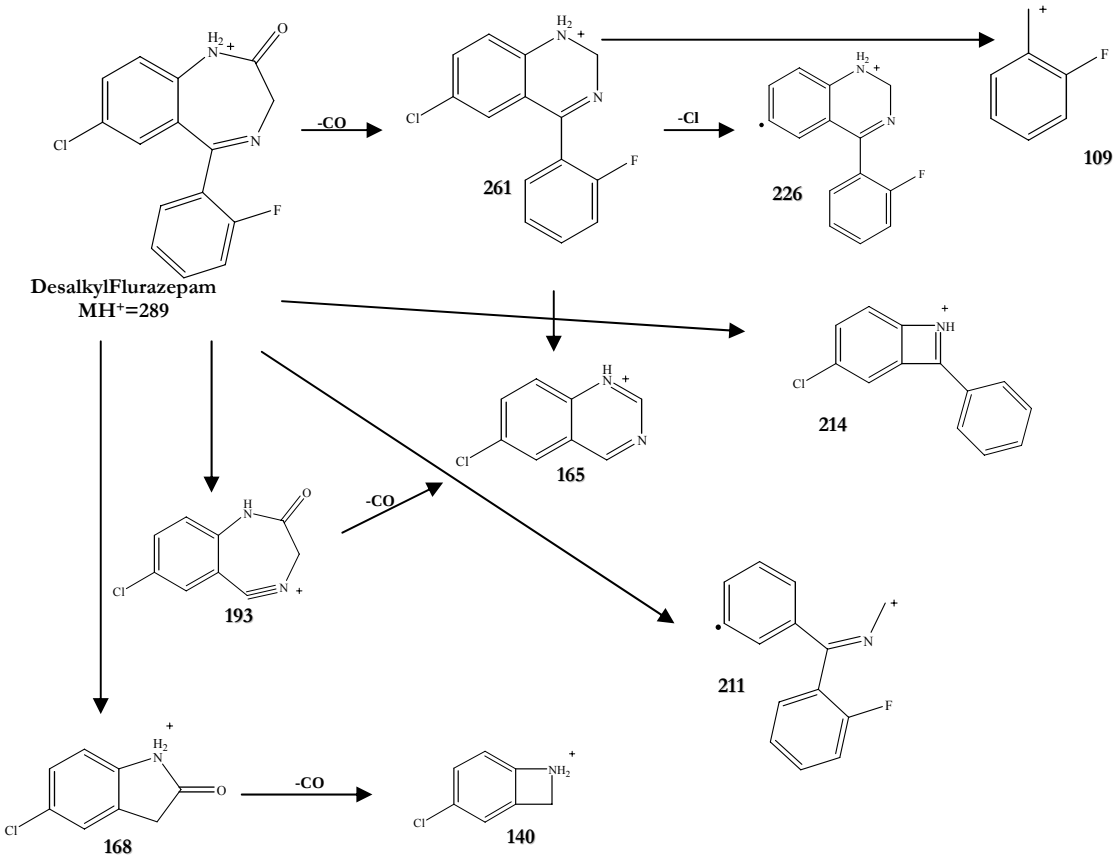

DesalkylFlurazepam

After electrospray ionization, the collisional activation of the protonated molecule induces loss of CO under rearrangement of the diazepine ring to a 1,2-dihydro-pyrimidine ring. The resulting fragment in turn falls apart into three main fragments. The first fragment is due to the loss of the fluoro-benzene group $[MH - CO - Ph(F)]^+$. A second fragment is due to the loss of a chorine atom $[MH - CO - Cl]^+$ and the last fragment is the fluoro-toluene group. A competitive fragmentation pathway assumes a first loss of the benzene group from the protonated molecule which in turn gives a fragment due to the loss of CO $[MH - Ph - CO]^+$. Another step is the loss of benzonitrile from the protonated molecule which in turn gives a fragment due to the loss of CO $[MH - PhCN(F) - CO]^+$, O=C=NH, Chlorine $[MH - O=C=NH -Cl]^+$, and NH_2COCH_3 with Fluorine $[MH - NH_2COCH_3 - F]^+$. The energy resolved plots show that the curves of the fragments obtained from the loss of benzene and chlorine groups, after the CO loss, increase with the fragmentation energy until a plateau at around 20 eV is reached. In contrast, the formation of the other main fragments are unaffected by the fragmentation energy. The toluene group and the fragment $[MH - PhCN(F) - CO]^+$ are the only fragments which show an exponential growth when the energy increases.

4.12 Group III: Flunitrazepam

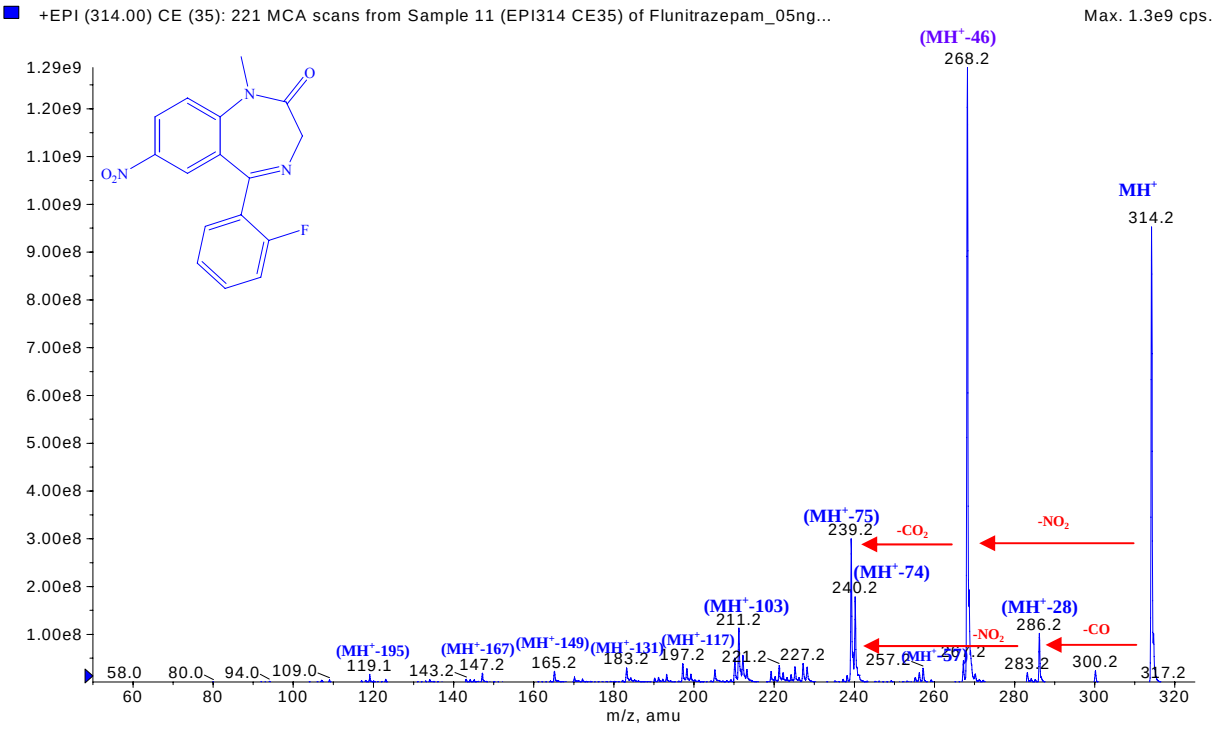

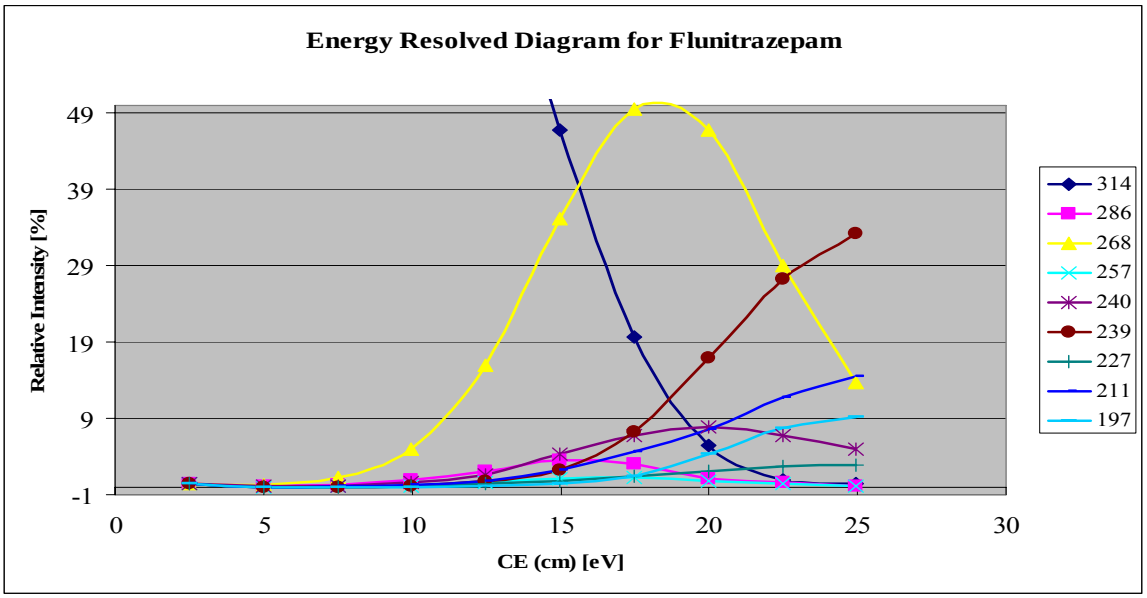

Fragmentation Pathway Proposal for Flunitrazepam

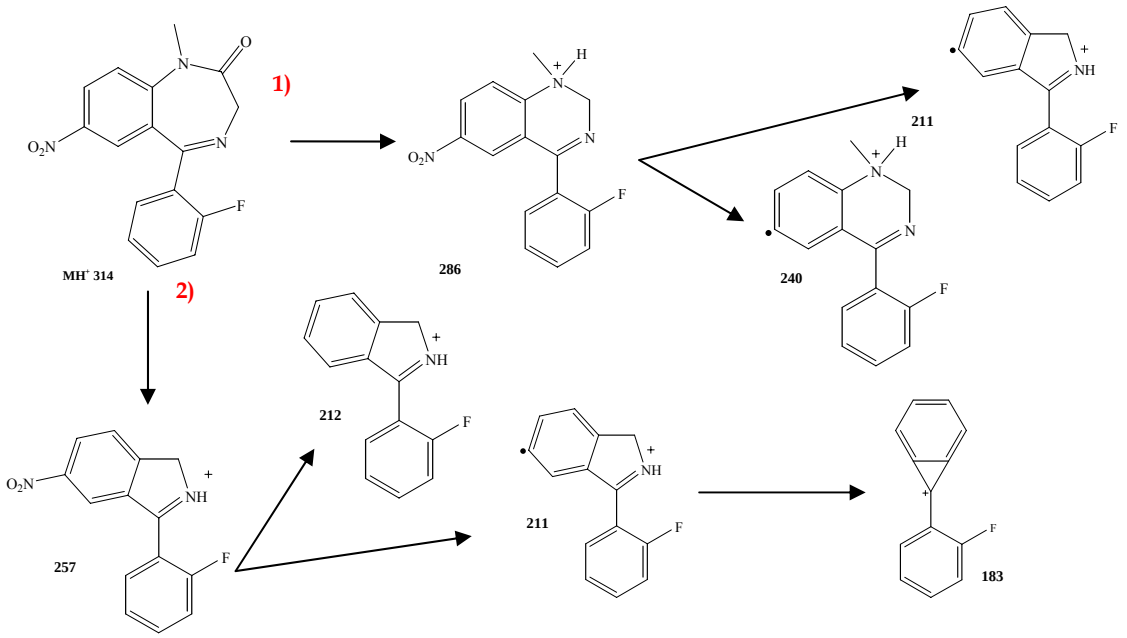

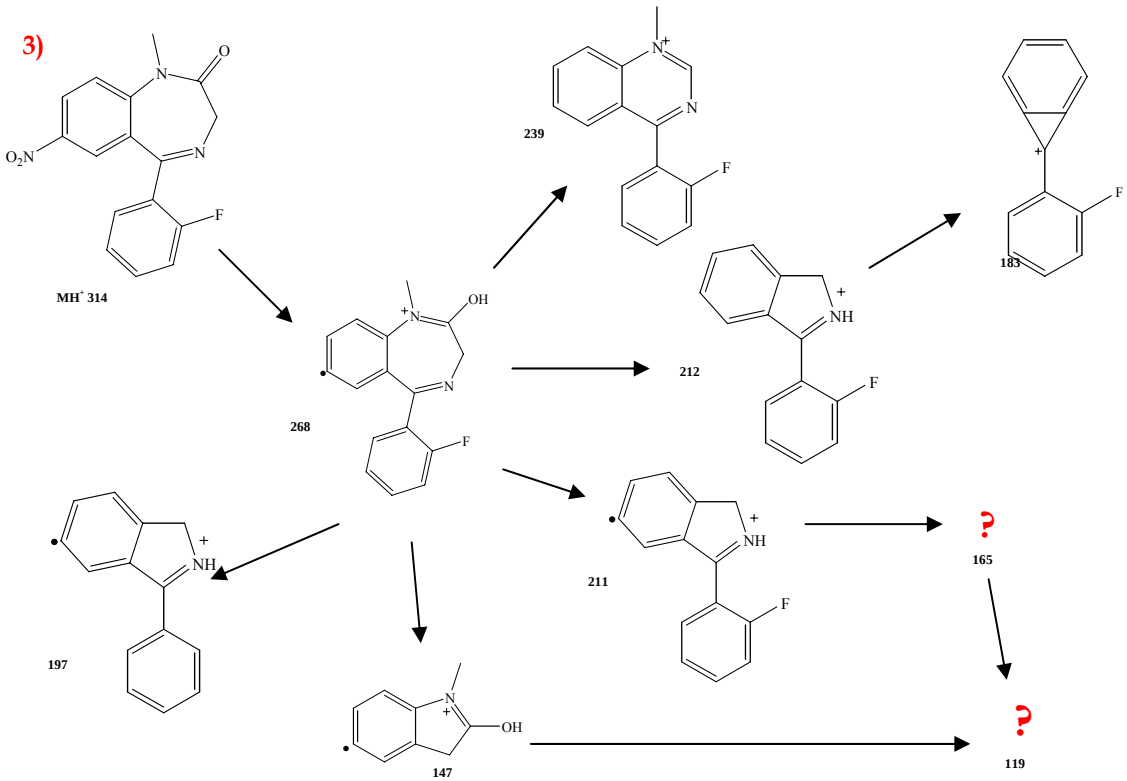

Flunitrazepam

After electrospray ionization, the collisional activation of the protonated molecule induces loss of CO followed by rearrangement of the diazepine ring to a 1,2-dihydro-pyrimidine ring. The resulting fragment in turn decomposes into two main fragments with the loss of NO_2 $[MH - CO - NO_2]^+$and HCN $[MH - CO - HCN]^+$. A competitive collision step of the protonated molecule induces a primary loss of NO_2. The resulting fragment in turn decomposes into five main fragments which constitute the greater part of the fragmentation. The loss of an $O=C=NCH_3$ group causes a further rearrangement of the 1,2-dihydro-pyrimidine ring to a pyrrole ring $[MH - NO_2 - O=C=NCH_3]^+$, whereas further fragments are due to the loss of a benzonitrile group $[MH - NO_2 - PhCN(F)]^+$ and CO $[MH - NO - CO]^+$. Other fragments are due to the loss of CO, HCN $[MH - CO - O=C=NCH_3]^+$ and CO, HCN, fluorine atom $[MH - NO2 - CO - HCN - F]^+$. Another competitive fragmentation pathway assumes a first loss of $O=C=NCH_3$ $[MH - O=C=NCH_3]^+$ and a loss of CO and HCN $[MH - CO - HCN]^+$ from the protonated molecule which in turn gives another fragment due to another loss of HCN $[MH - CO - HCN - HCN]^+$. The energy resolved plots show that the curves of the fragments obtained from the loss of CO, $O=C=NCH_3$, and CO and HCN, after the NO_2 loss, increased with the fragmentation energy. In contrast, the formation of the other main fragments seem unaffected by the fragmentation energy. The 119 group is the only fragment which shows an exponential growth when the energy increases.

4.13 Group III: Flurazepam

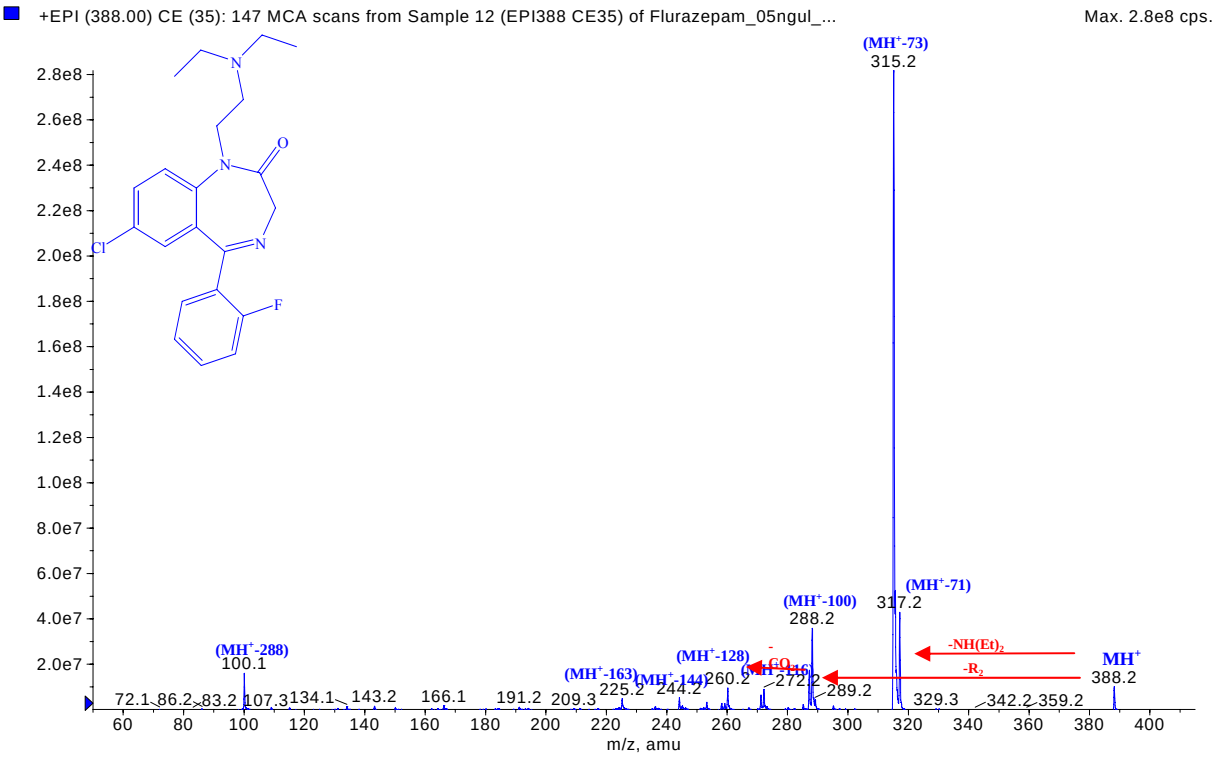

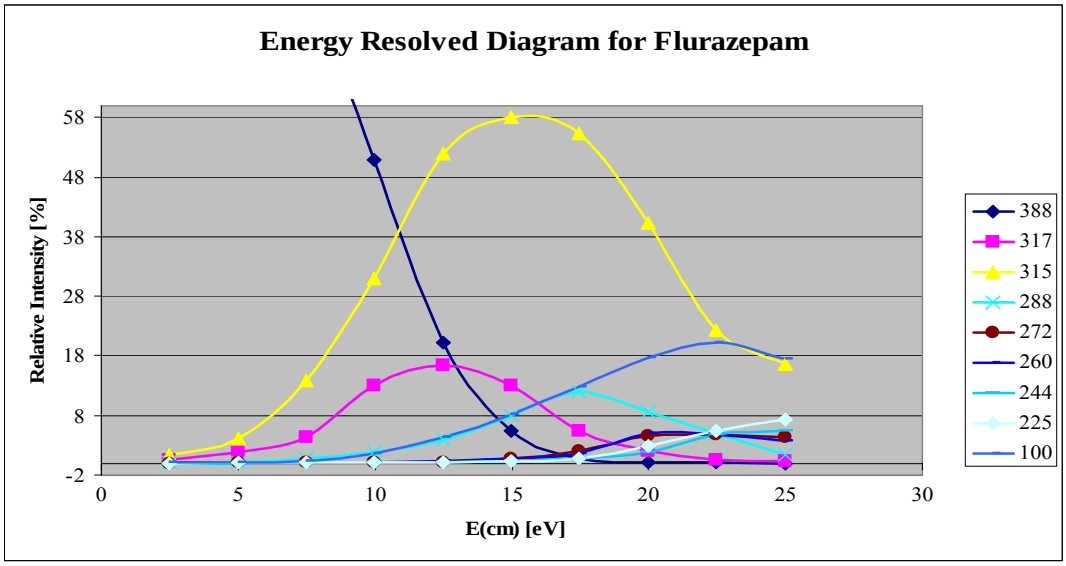

Fragmentation Pathway Proposal for Flurazepam

1)

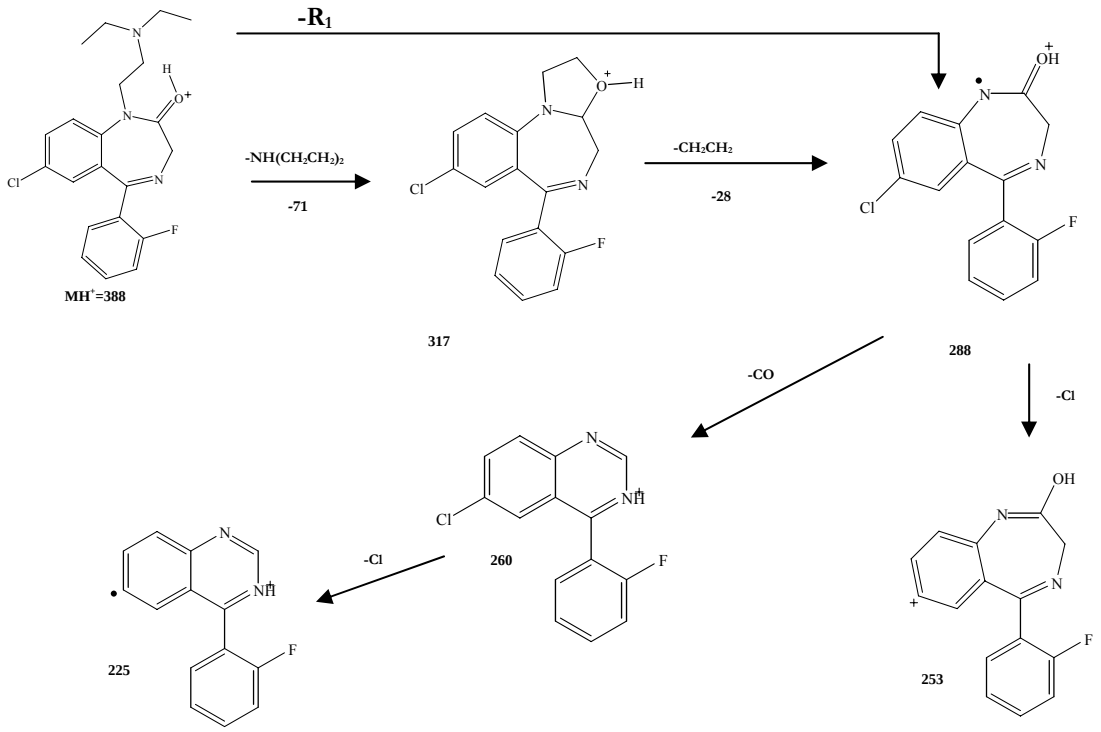

2)

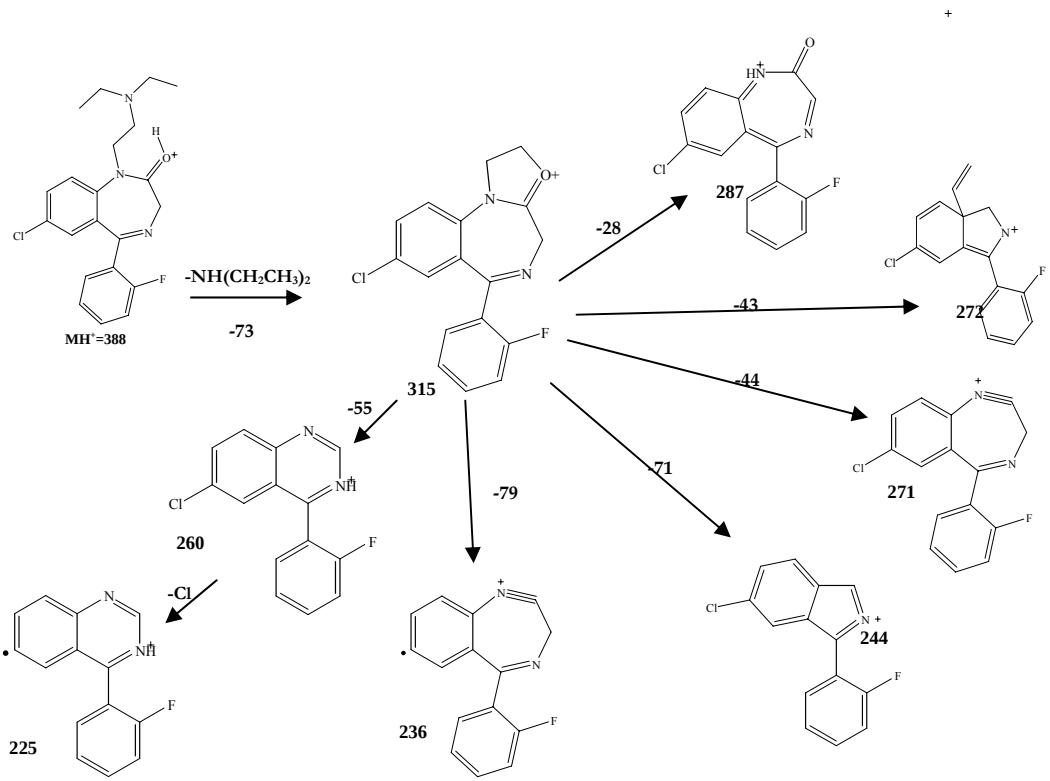

Flurazepam

After electrospray ionization, the collisional activation of the protonated molecule induces loss of the R_1 group, in one or two steps. After that, loss of chlorine $[MH - R_1 - Cl]^+$or CO $[MH - R_1 - CO]^+$and then the chlorine$[MH - R_1 - CO - Cl]^+$ can take place. A competitive fragmentation pathway assumes a first loss of a part of R_1: $NH(CH_2CH_3)_2$, with the rearrangement to a new structure containing three fused cycles. The resulting fragment in turn decomposes into six main fragments which constitute the greater part of the fragmentation. The first fragment is due to the loss of $CH_2COCHCH$ (Cycle), with the rearrangement to a 1,2-dihydro-pyrimidine ring. From this fragment further loss of chlorine $[MH - NH(CH_2CH_3)_2 - CH_2COCHCH]^+$ is possible. Another fragment is due to the loss of a $NHCHCHCH_2O$ (cycle) group which causes a further rearrangement to a pyrrole ring $[MH - NH(CH_2CH_3)_2 - NHCHCHCH_2O]^+$. Another fragment is due to the loss of a $O=C=CH_2$ group $[MH - NH(CH_2CH_3)_2 - O=C=CH_2]^+$, or to the sequential loss of this group and chlorine $[MH - NH(CH_2CH_3)_2 - O=C=CH_2 - Cl]^+$. Other fragments are due to the loss of an ethene group $[MH - NH(CH_2CH_3)_2 - CH_2=CH_2]^+$ and $O=CHCH_3$ $[MH - NH(CH_2CH_3)_2 - O=CHCH_3]^+$. The energy resolved plots show that the curves of the fragments obtained from the loss of CO and chlorine groups, after R_1 loss, increase with the fragmentation energy. A curve due to the loss of $NHCHCHCH_2O$ (cycle) group and the loss of $O=CHCH_3$ after the loss of $NH(CH_2CH_3)_2$ are also shown. In contrast, the formation of the other main fragments are unaffected by the fragmentation energy.

4.14 Group IV

4.15 Group IV: Alprazolam

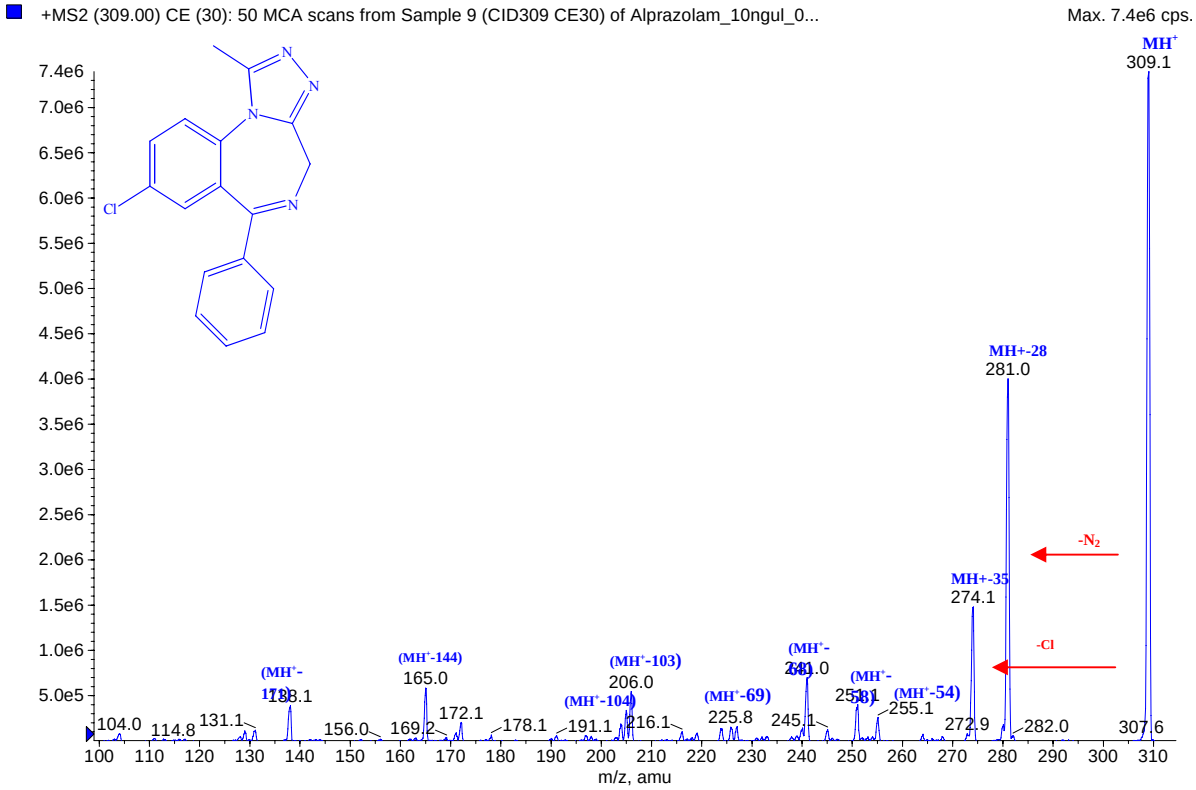

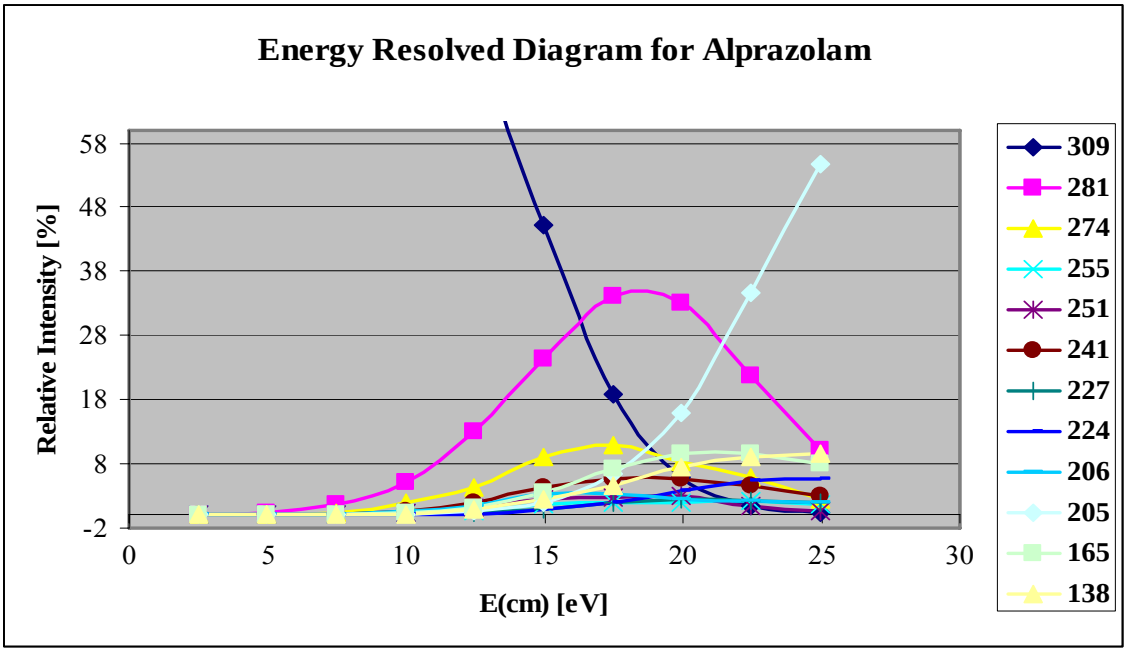

Fragmentation Pathway Proposal for Alprazolam

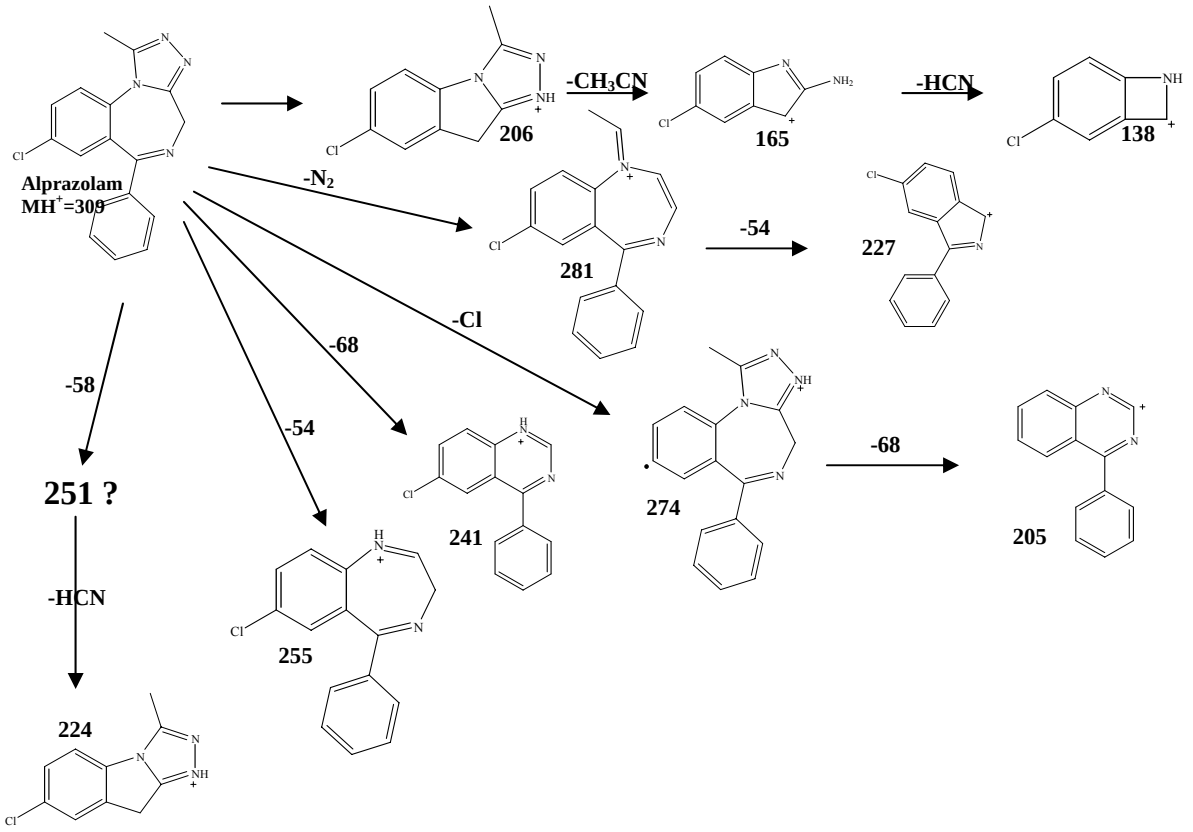

Alprazolam

After electrospray ionization, collisional activation of the protonated molecule induces the formation of six fragments. Among these fragments one is due to the loss of $CH_2CHCHNNCO$ (cycle) with the rearrangement of the diazepine ring to a 1,2-dihydro-pyrimidine ring. Another fragment is due to the loss of a N_2 $[MH -N_2]^+$ from which the CH_2NCHCH (cycle) $[MH -N_2 -CH_2NCHCH]^+$ is lost. In addition fragments due to the loss of a benzonitrile group $[MH - PhCN]^+$, from which the loss of CH_3CN $[MH - PhCN - CH_3CN]^+$ and then the loss of HCN $[MH - PhCN - CH_3CN -HCN]^+$ are observed. Other fragments are due to the loss of a chorine atom $[MH - Cl]^+$ and of N=NCH=CH (cycle) $[MH - N=NCH=CH]^+$. The energy resolved plots show that the curves of the fragments obtained from the loss of CH_3CN and the HCN groups, after the benzonitrile loss, increase with the fragmentation energy. In contrast, the formation of the other main fragments are unaffected by the fragmentation energy.

4.16 Group IV: Triazolam

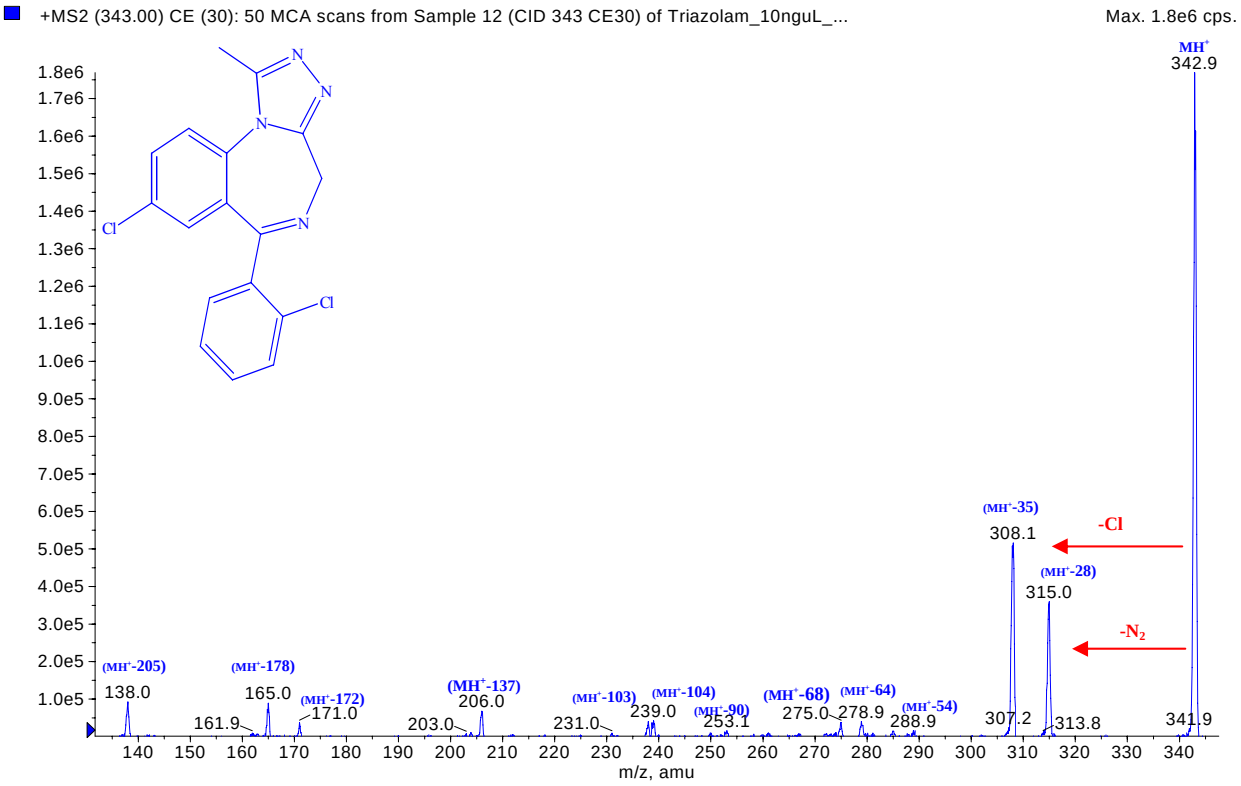

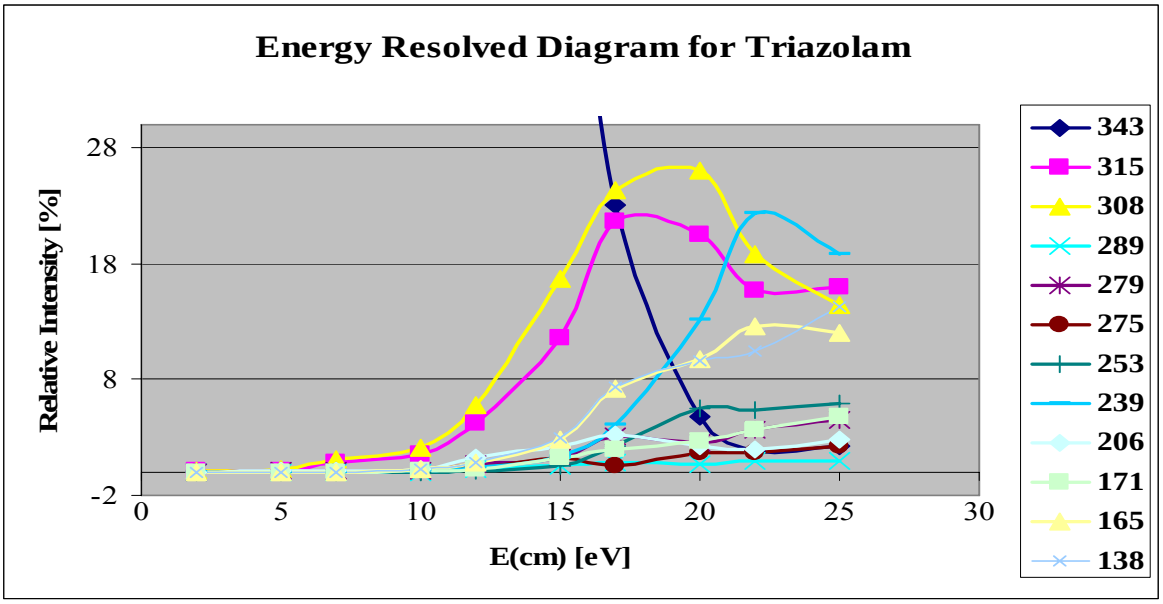

Fragmentation Pathway Proposal for Triazolam

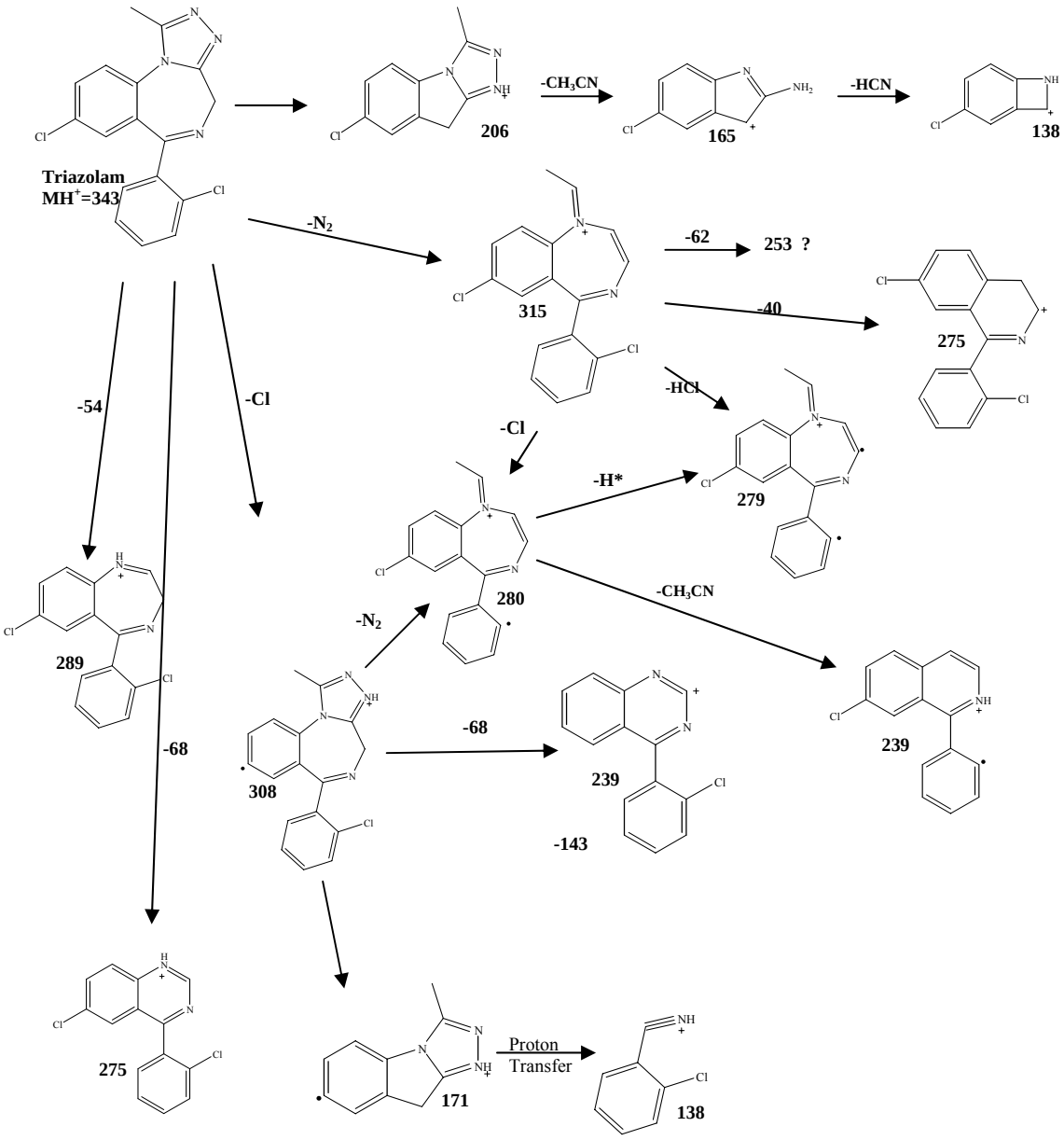

Triazolam

The collisional activation of the protonated molecule induces the formation of six fragments, that represent the main part of the fragmentation. One of these fragments is due to the loss of $CH_2CHCHNNCO$ (cycle) with the rearrangement of the diazepine ring to a 1,2-dihydro-pyrimidine ring. Another fragment is due to the loss of a N_2 $[MH –N_2]^+$, from which the loss of NHCHCH $[MH –N_2 -NHCHCH]^+$, or HCl $[MH –N_2 -HCl]^+$ or chlorine $[MH –N_2 -Cl]^+$. From this last one the loss of CH_3CN $[MH –N_2 –Cl –CH_3CN]^+$ is shown, whereas a fragment due to the loss of a benzonitrile group $[MH – PhCN(Cl)]^+$, can fragment further by loss of CH_3CN $[MH – PhCN(Cl) – CH_3CN]^+$ followed by HCN $[MH – PhCN(Cl)– CH_3CN – HCN]^+$. Other fragments are due to the loss of a chorine atom $[MH – Cl]^+$, followed by loss of benzonitrile $[MH – Cl –PhCN(Cl)]^+$, or of $N=NCH_2CH=CH$ (cycle) $[MH –Cl -N=NCH_2CH=CH]^+$ with the rearrangement to a 1,2-dihydro-pyrimidine ring. The loss of N_2 $[MH –Cl – N_2]^+$, and followed by N=NCH=CH (cycle) $[MH – N=NCH=CH]^+$ is also possible. The energy resolved plots show that the curves of the fragments obtained from the loss of CH_3CN and HCN groups, after the benzonitrile loss, and the curve obtained from the loss of $N=NCH_2CH=CH$ group after the chlorine loss, increase with the fragmentation energy. In contrast, the formation of the other main fragments are unaffected by the fragmentation energy.

4.17 Group IV: Midazolam

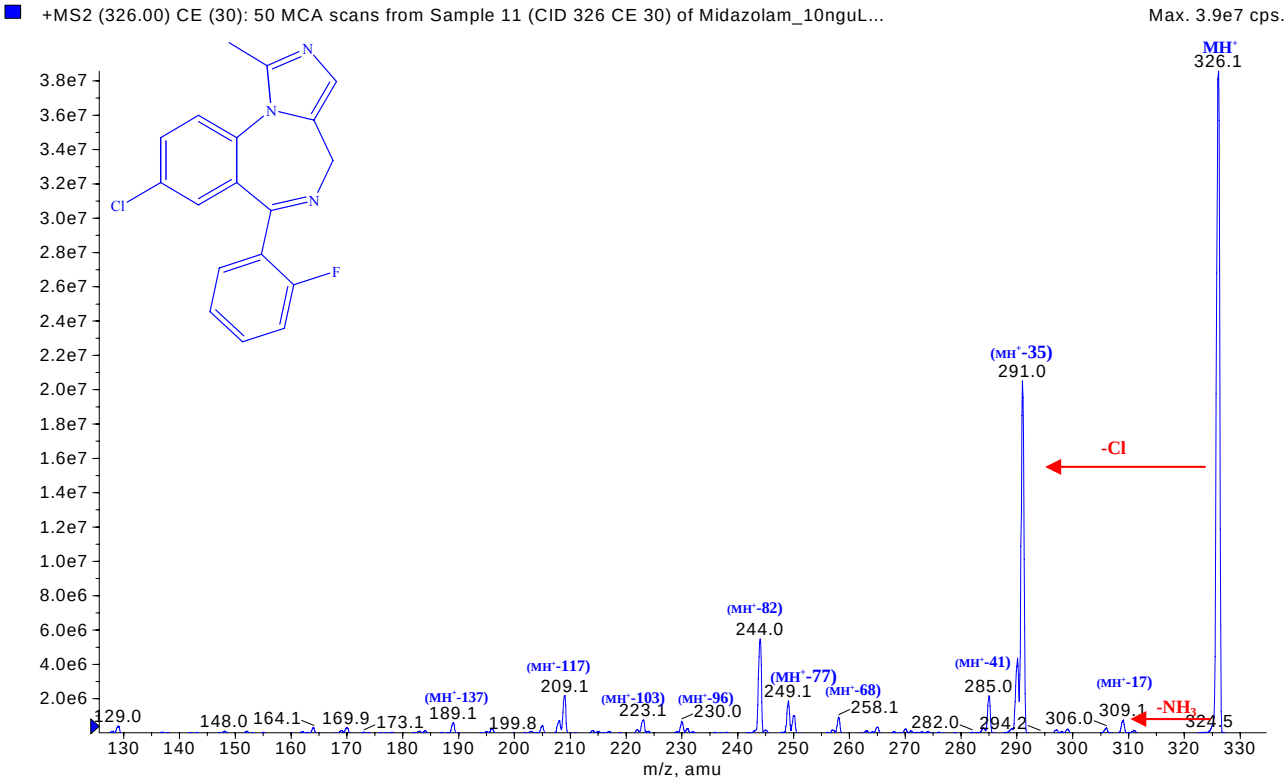

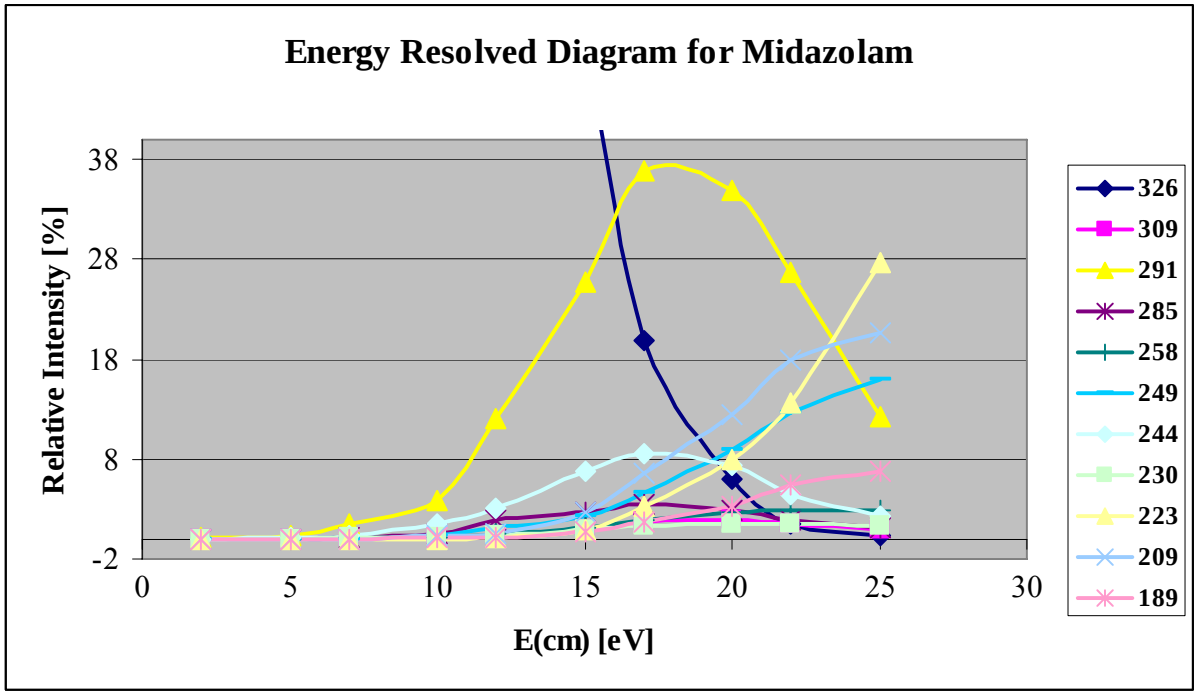

Fragmentation Pathway Proposal for Midazolam

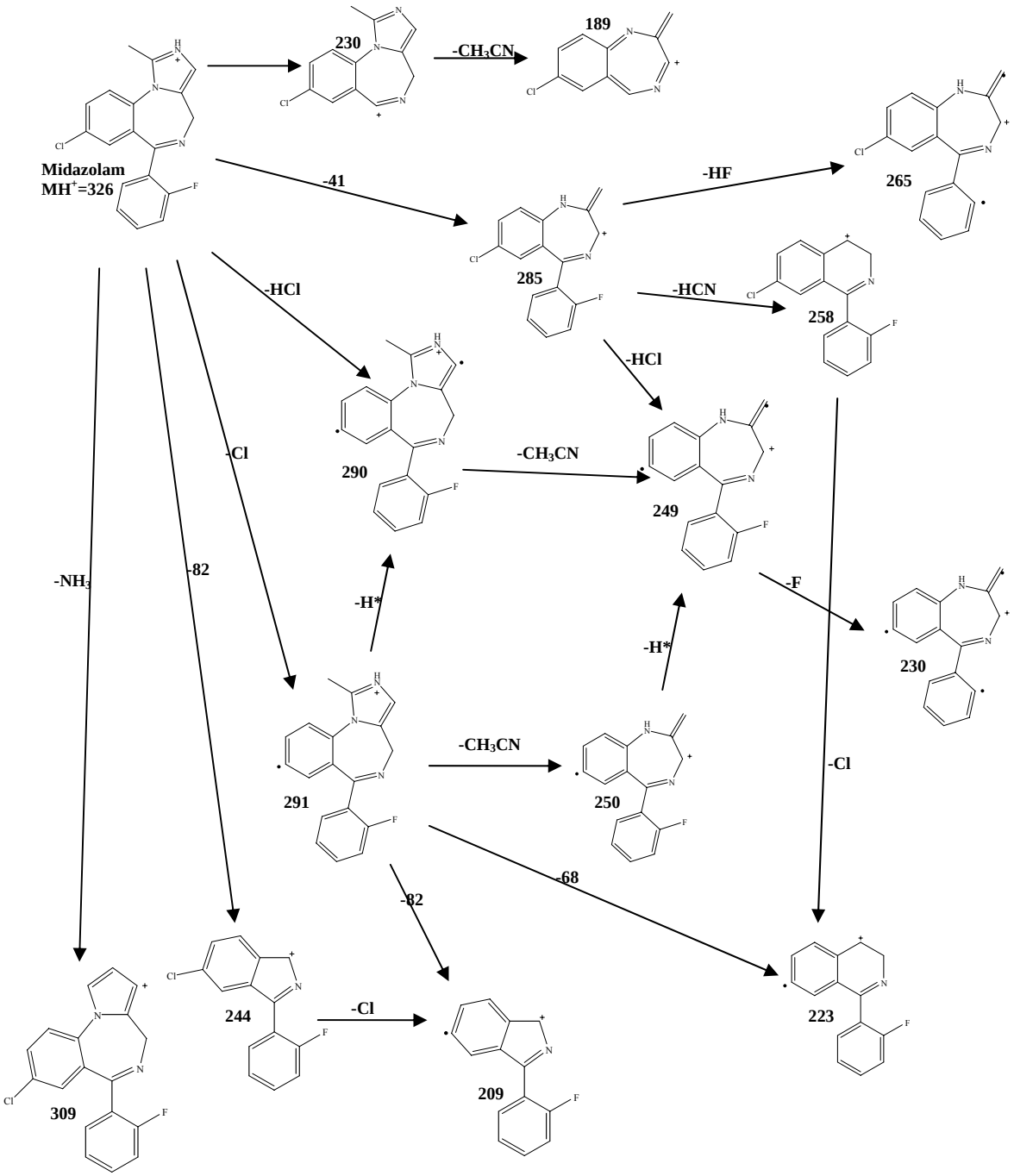

Midazolam

The collisional activation of the protonated molecule results in the formation of six fragments, that represent the main part of the fragmentations. One of these fragments is due to the loss of $CH_3CHNNCH$ (cycle) group which causes a further rearrangement to a pyrrole ring $[MH - CH_3CHNNCH]^+$ which in turn can easily lose a chlorine $[MH - CH_3CHNNCH - Cl]^+$. One of the fragments is due to the loss of a benzene group $[MH - Ph]^+$, followed by CH_3CN $[MH - Ph - CH_3CN]^+$. Others fragments are due to the loss of NH_3 $[MH - N_3]^+$, chlorine $[MH - Cl]^+$, HCl $[MH - HCl]^+$, from which loss of CH_3CN follows $[MH - HCl - CH_3CN]^+$, which can fragment further by loss of Fluorine $[MH - HCl - CH_3CN - F]^+$. After the loss of chlorine a number of fragmentations were observed, including the loss of CH_3CN $[MH - Cl - CH_3CN]^+$, $CH_3CHNNCH$, which causes a further rearrangement to a pyrrole ring $[MH - Cl - CH_3CHNNCH]^+$, or N=NCH=CH (cycle) with a rearrangement to a 1,2-dihydro-pyrimidine ring $[MH - Cl - N=NCH=CH]^+$. The last fragment is due to the loss of CH_3CN $[MH - CH_3CN]^+$, from which a loss of HF $[MH - CH_3CN - HF]^+$, HCl $[MH - CH_3CN - HCl]^+$ can be observed. This last fragment can also give a loss of fluorine $[MH - CH_3CN - HCl - F]^+$, and HCN $[MH - CH_3CN - HCN]^+$, which in turn fragments further under loss of chlorine $[MH - CH_3CN - HCN - Cl]^+$. The energy resolved plots show that the curves of the fragments obtained from the loss of CH_3CN , after the HCl loss, and the curve obtained from the loss of $N=NCH_2CH=CH$ group after the chlorine loss, increase with the fragmentation energy. In contrast, the formation of the other main fragments are unaffected by the fragmentation energy.

We can reassume that CID (Collision Induced Dissociation) analysis of the benzodiazepines studied showed that the first fragmentation is the loss of CO. In addition Group I shows also loss of a benzonitrile group, while Group II shows loss of H_2O followed by loss of benzonitrile or benzene. In Group III, Flurazepam shows a different fragmentation process, but after loss of the substituent in position R_1, a common fragmentation pathway is shown with loss of CO followed by loss of the substituent in position R_4.

In the Group IV the situation seems more complicated because these molecules have no CO group, but another ring structure, containing one or two Nitrogen atoms fused with the benzodiazepine ring. In this case, the first fragmentation observed is the loss of N_2 or NH_3, depending on the number of Nitrogens; in addition loss of benzonitrile, and then of CH_3CN, from the parent peak, as well as the loss of Chlorine and then the loss of a

fragment with m/e 68 is observed. A common pathway observed in every kind of benzodiazepine is a rearrangement of the diazepine ring to a 1,2-dihydro-pyrimidine ring.

This fragmentation study offers the possibility of creating a mass spectral library for benzodiazepine drugs. This library could be useful for the identification of these drugs in clinical and forensic samples. The knowledge of significant peaks in the mass spectra can be very useful for identification of benzodiazepines.

The extensive use of variation of the fragmentation energy allowed detailed breakdown curves, which could be used to optimize the fragmentation pattern for each drug.

References

[1] M.C.A.Costa, A.C.Gaudio, Y.Takahata, J.Mol.Struct. 394(1997)291-300

[2] B. Hemmateenejad, R. Miri, M. Akhond, M. Shamsipur, Chemom. Intel. Lab. Systems. 64 (2002) 91-99

[3] E. Vigneau, M. Devaux, M. Qannari, P. Robert, J. Chemom. 11 (1997) 239.

[4] D. Massart, B. Vandeginste, L. Buydens, S. De Jong, P. Lewi, J. Smeyers-Verbeke, Handbook of Chemometrics and Qualimetrics, Elsevier, Amsterdam, 1998.

[5] B. Lavine, Anal. Chem. 72 (2000) 91R.

[6] D. Haaland, Appl. Spectrosc. 54 (2000) 246.

[7] T. Feam, J. Near Infrared Spectrosc. 9 (2001) 229.

[8] R. Brereton, Chemometrics, Data Analysis for the Laboratory and Chemical Plant, Wiley, Chichester, 2003.

[9] P. Geladi, Spectrochim. Acta Part B 58 (2003) 767.

[10] D.M. Haaland, E.V. Thomas, Anal. Chem. 60 (1988) 1193.

[11] P. Peralta-Zamora, A. Kunz, N. Nagata, R.J. Poppi, Talanta 47 (1988) 77.

[12] D. Haaland, E. Thomas, Anal. Chem. 62 (1990) 1091.

[13] K.N. Andrew, P.J. Worsfold, Analyst 119 (1994) 1541.

[14] I. Duran-Meras, M. de la Pena, A. Espinosa-Mansilla, F. Salinas, Analyst 118 (1993) 807.

[15] J.J. Berzas Nevado, J. Rodriguez Flores, M.J. Villaseñor Llerena, N. Rodriguez Farinas, Talanta 48 (1999) 895.

[16] M. Blanco, J. Coello, F. Gonzales, H. Itturiaga, S. Maspoch, X. Tomas, J. Pharm. Biom. Anal. 12 (1994) 509.

[17] B.W. Glombitza, P.C. Schimdt, J. Pharm. Sci. 83 (1994) 751.

[18] R.D. Bautista, F.J. Aberasturi, A.I. Jimenez, Talanta 43 (1996) 2107.

[19] J.J. Berzas Nevado, J. Rodriguez Flores, G. Castañeda Peñalvo, Anal. Chim. Acta 340 (1997) 257.

[20] A. Navalon, R. Blanc, M. del Olmo, J.L. Vilchez, Talanta 48 (1999) 469.

[21] H. Martens, T. Naes, Multivariate Calibration, Wiley, Chichester, 1989.

[22] H. Wold, Research Papers in Statistics, Wiley, New York, 1996, p. 411.

[23] H. Wold, H. Martens, S. Wold, in: A. Ruhe, B. Kagstrom (Eds.), Multivariate Calibration Problems in Chemistry Solved by PLS, Heidelberg, 1983, pp. 286–293.

[24] K.R. Beebe, B.R. Kowalski, Anal. Chem. 59 (1987) 1007.

[25] S. Wold, P. Geladi, K. Esbensen, J. Ochaman, J. Chemom. 41 (1987) 1.

[26] A. Garrido Frenich, D. Jouan-Rimbaud, D.L. Massart, S. Kuttatharmmakul, M. Martinez Galera, J.L. Martinez Vidal, Analyst 120 (1995) 2787.

[27] L. YI-Zieng, X. Yu-Long, Y. Ru-Quin, Anal. Chim. Acta 222 (1989) 347.

[28] M.S. Linares, J.M.G. Fraga, A.I. Jimenez, F. Jimenez, J.J. Arias, Anal. Lett. 32 (1999) 2489.

[29] R. Todeschini, D. Galvegni, J.L. Vilchez, M. del Olmo, N. Navas, Trends Anal. Chem. 18 (1999) 93.

[30] C. Vetuschi, G. Ragno, Anal. Lett. 33 (2002) 559.

[31] O.J. Sichelschmind, C. Hahnefeld, T. Hohlfeld, F.W. Herberg, K. Schrör. *Cardiovascular Research* 58 (2003) 602-610.

[32] K. Büyükafşar, A. Yazar, D. Düşmez, H. Öztürk, G. Polat and A. Levent. *Pharmacological Research* Vol. 44 No 4, 2001.

[33] A. Hirayama, K. Kodama, Y. Yui, H. Nonogi, T. Sumiyoshi, H. Origasa, S. Hosoda and C. Kawai, for the JMIC-M Investigators. *Am J Cardiol* 2003; 92 : 789-793.

[34] R.M. Smith. *Journal of Chromatography A*, 1000 (2003) 3 – 27.

[35] E.P.C. Lai, S.G. Wu. *Analytica Chimica Acta*, 481 (2003) 165 – 174.

[36] M. Jelikic-Stankov, J. Odovic, D. Stankov, P. Djurdjevic. *Journal of Pharmaceutical and Biomedical Analysis*, 18 (1998) 145 – 150.

[37] M[a] I. Pascual-Reguera, G. Pérez Parras, A. Molina Díaz. *Microchemical Journal*, 77 (2004) 79 – 84.

[38] A. Schellen, B. Ooms, D. van de Lagemaat, R. Vreeken, W.D. van Dongen. *Journal of Chromatography B*, 788 (2003) 251 – 259.

[39] S. Harder, P.A. Thürmann, A. Hellstern & A. Benjaminov. *British Journal of Clinical Pharmacology*, Vol. 42, 4 (1996) 443.

[40] T. D. McLaren, J.Brodbelt, *Anal. Chem*. **1993** *65*,2380-2388.

[41] S. Bourcier, Y.Hoppilliard, T. Kargar-Grisel, J.M.Pechinè, F.Perez, *Eur. J. Mass Spectrom*. **2001** *7*, 359-371.

[42]W. F. Smyth, S.McClean, V.N.Ramachandran, *Rapid Commun. Mass Spectrom*. **2000** *14*, 2061-2069.

[43] W. F. Smyth, *Analytica Chimica Acta* **2003**, *492*, 1-16.

[44] W. F. Smyth, C.Joyce, V.N.Ramachandran, E.O'Kane, D.Coulter, *Analytica Chimica Acta* **2004**, *506*, 203-214.

[45] T. Gunnar, K.Ariniemi, P.Lillsunde, *J. Chromatogr. B* **2005** *818* 175-189.

[46] A.G.A.M. Lips, W.Lamejer, R.H.Fokkens, N.M.M.Nibbering, *J. Chromatogr.* **2001**, *B* 759, 191-207.

[47] J.B.Y. Cheng, K.W.M. Siu, A.C. Hopkinson, Fragmentations of Diazepams, poster ASMS conference, San Antonio, 4-10 June, 2005.